

INVESTIGATION OF CO AND CO₂ EMISSIONS FROM A DOMESTIC GAS BURNER

**A Thesis Submitted to
the Graduate School of Engineering and Sciences of
İzmir Institute of Technology
in Partial Fulfillment of the Requirements for the Degree of**

MASTER OF SCIENCE

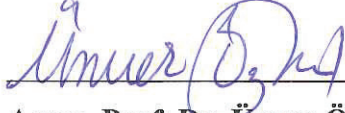
in Mechanical Engineering

**by
Alpay ÖZSÜER**

**May 2019
İZMİR**

We approve the thesis of **Alpay ÖZSÜER**

Examining Committee Members:



Assoc. Prof. Dr. Ünver ÖZKOL

Department of Mechanical Engineering, İzmir Institute of Technology



Assoc. Prof. Dr. Erdal ÇETKİN

Department of Mechanical Engineering, İzmir Institute of Technology



Assoc. Prof. Dr. Nurdan Yıldırım ÖZCAN

Department of Mechanical Engineering, Yaşar University

27 May 2019



Assoc. Prof. Dr. Ünver ÖZKOL

Supervisor, Department of Mechanical
Engineering, İzmir Institute of
Technology



Prof. Dr. Sedat AKKURT

Head of Department of Mechanical
Engineering

Prof. Dr. Aysun SOFUOĞLU

Dean of Graduate School of
Engineering and Science

ACKNOWLEDGMENTS

First, I would like to thank to my former advisor, Assist. Prof. Dr. Alvaro Diez for his continuous support and understanding. I have gained the ability to search for and reach to the information under his guidance. It would be impossible without his patience throughout my master's degree.

I would also like to thank to my advisor Assoc. Prof. Dr. Ünver Özkol, for his great support. In a crucial period, he helped me finalize my thesis with his guidance.

I would like to express my gratitude to my friends, Burak Karakaya, Dr. José Salvador Ochoa Torres, Erdem Sevgen and Serkan Emre Erfidan, from Bosch and Siemens Home Appliances Group. Whenever I needed their support, they have always been there for me as friends, rather than as colleagues.

I would especially like to thank to my dearest friend Abdullah Asil Atay, who has been doing his master's degree in computer engineering department in same period. His endless support and encouragement helped me from first second to the last.

Finally, I would like to thank to my dear mother Filiz Telli. Nothing would be possible without her existence.

ABSTRACT

INVESTIGATION OF CO AND CO₂ EMISSIONS FROM A DOMESTIC GAS BURNER

In this study, performance of a domestic gas burner from a gas cooktop will be evaluated. Compared to the induction and radiant cooktops, gas cooktops are less efficient, and they cause indoor air pollution. Air pollution is a global hot topic and fossil fuels are one of the biggest sources of it. Natural gas is widely used throughout the world and with this wide usage, gas cooktops are still preferred since it is also cheaper than electricity in some countries. Even though air pollution is a hot topic, the lack of indoor air quality regulations makes pollutant emissions from gas sources dangerous to human health. Even if a small improvement in efficiency or pollutant emission rate is performed, it will lead to a large impact on the global natural gas consumption or global air pollution.

The aim of this study is to see effects of changing loading height on domestic gas burners. To make observations, experimental studies, which will be supported by numerical studies, will be performed according to requirements of European Norm.

ÖZET

EV TİPİ SETÜSTÜ OCAK BRULÖRLERİNDE CO VE CO₂ SALINIMININ İNCELENMESİ

Bu çalışmada, setüstü ocaklarda kullanılan ev tipi bir gaz brulörünün performansı incelenecektir. İndüksiyon ve radyant setüstü ocaklar ile kıyaslandığında, gazlı setüstü ocaklar daha az verimlidir ve iç hava kirliliğine sebep olur. Hava kirliliği dünya çapında gündemde olan bir konu ve fosil yakıtlar bunun en önemli sebeplerinden biri. Doğal gaz dünyada geniş çapta kullanılıyor ve yaygın kullanımla birlikte elektriğe göre bazı ülkelerde daha ucuz olması, gazlı ocakları da hâlâ tercih sebebi yapıyor. Hava kirliliğinin dünya çapında gündem konusu olmasına rağmen, iç hava kalitesi ile ilgili düzenlemelerin eksikliği, atık çevre kirleticiler maddelerin insan sağlığına zarar verme riskini beraberinde getiriyor. Bu sebeple, gazlı ocakların verimliliğinde veya atık çevre kirleticiler madde salınım oranında küçük bir iyileştirme bile yapılırsa, küresel doğal gaz kullanımına veya küresel hava kirliliğine olumlu yönde büyük bir etkisi olacaktır.

Bu çalışmanın amacı, değişik tencere yükleme yüksekliklerinin, ev tipi bir gaz brulöründeki etkilerini görmektir. İncelemeleri yapmak için, Avrupa Normu'na uygun şekilde, sayısal çalışmalarla desteklenecek olan, deneysel çalışmalar yapılacaktır.

TABLE OF CONTENTS

LIST OF FIGURES.....	viii
LIST OF TABLES.....	x
LIST OF SYMBOLS.....	xi
CHAPTER 1 INTRODUCTION.....	1
CHAPTER 2 LITERATURE SURVEY.....	3
2.1. Field Studies.....	3
2.2. Experimental and Numerical Studies.....	5
CHAPTER 3 METHODOLOGY.....	13
3.1. Combustion Definition.....	14
3.1.1. Flame.....	14
3.1.1.1. Premixed Flame.....	15
3.1.1.2. Diffusion Flames.....	16
3.1.2. Fuel.....	17
3.1.3. Flammability.....	18
3.1.4. Minimum Ignition Energy.....	18
3.1.5. Laminar Flame Speed.....	19
3.2. Experimental Setup.....	19
3.2.1. Background Information.....	20
3.2.2. Tests.....	22
3.2.2.1. Heat Input.....	23
3.2.2.2. Combustion Test.....	24

3.2.2.3. Efficiency Test.....	27
3.3. Numerical Background	29
3.3.1. Ideal Gas and Conservation of Mass	29
3.3.2. Combustion Stoichiometry and Equivalence Ratio.....	31
3.3.3. Enthalpy and Enthalpy of Formation	33
3.3.4. Adiabatic Flame Temperature	36
3.3.5. Numerical Modeling.....	39
CHAPTER 4 RESULTS AND DISCUSSIONS	45
4.1. Preliminary Results and Model Validation.....	45
4.1.1. Effects of Pan Support and Hob Sheet Design	48
4.1.2. Effect of Reduced Reaction Mechanism	50
4.2. Mesh Dependency.....	52
4.3. Effects of Loading Height.....	53
CHAPTER 5 CONCLUSION AND FUTURE WORK.....	57
REFERENCES	59

LIST OF FIGURES

<u>Figure</u>	<u>Page</u>
Figure 2.1. Change in CO emission and efficiency against loading height at different thermal inputs, provided by fuel regulator opening angle (Source: [8]).....	6
Figure 2.2. Change in thermal efficiency with varying burner power for different burner types (Source: [10]).....	8
Figure 2.3. Results of thermal efficiency for different flow rates (Source: [11]).....	9
Figure 2.4. Results of a) cooking efficiency b) annual energy cost for cooker and pan types (Source: [14]).....	11
Figure 3.1. Flow chart of experimental and numerical studies.....	13
Figure 3.2. Premixed flame model (Source: [18]).....	15
Figure 3.3. Premixed Flame Reaction and Post Flame Zones.....	16
Figure 3.4. Diffusion Flame Model (Source: [18]).....	17
Figure 3.5. Cooktop model.....	20
Figure 3.6. An example of configuration.....	20
Figure 3.7. Section of a cooktop burner.....	21
Figure 3.8. Schematic of adiabatic flame temperature (Source: [21]).....	36
Figure 3.9. Burner slice to create the domain.....	39
Figure 3.10. Domain with the taken slice. Trimetric and top views.....	40
Figure 3.11. Domain slice.....	40
Figure 4.1. Hood a) the usage in test and b) corresponding surface.....	46
Figure 4.2. Temperature distribution in the midplane of domain for methane combustion.....	47
Figure 4.3. Difference in hob design and pan support for appliances a) deep pool with 2-finger pan support b) narrow pool with 1-finger thin pan support.....	48
Figure 4.4. Difference in pan support a) 2-finger model b) 3-finger model.....	49
Figure 4.5. Change of CO concentrations with changing gas flow rate.....	51
Figure 4.6. Change of CO ₂ concentrations with changing gas flow rate.....	52
Figure 4.7. Loading Height.....	53
Figure 4.8. Change in thermal efficiency with loading height.....	53
Figure 4.9. Contour of pot surface heat flux.....	54

Figure 4.10. Heat flux distribution on bottom surface of the pot	55
Figure 4.11. Changes in CO ₂ and CO concentrations with loading height	55

LIST OF TABLES

<u>Table</u>	<u>Page</u>
Table 2.1. Nitrogen dioxide levels ($\mu\text{g}/\text{m}^3$) recorded in rooms with major nitrogen dioxide sources present in the house (Source: [6])	4
Table 3.1. Characteristics of the reference test gases (Source: [19]).....	22
Table 3.2. Test pressures for reference gases: 2H(G20) and 3B/P (G30) (Source: [19])	24
Table 3.3. Test conditions and maximum limit of CO concentration (Source: [19]).....	25
Table 3.4. Test conditions for different nominal heat input values (Source: [20]).....	27
Table 3.5. Enthalpy of formation (mass and molar) for some species at 298 K and 1 bar (Source: [16])	35
Table 3.6. Heat capacities of gases at 1000 K and 1 bar	38
Table 3.7. Change in numbers of cells between tetrahedral and polyhedral meshing for the domain	41
Table 3.8. Reactions for 2-step reduced mechanism in Fluent.....	43
Table 4.1. Water-free results from Fluent and experiment.....	47
Table 4.2. Combustion test results from appliance a and appliance b.....	48
Table 4.3. Efficiency test results from pan support a and pan support b with +/- %0.9 error tolerance from measurement uncertainties.....	49
Table 4.4. Mesh dependency	52
Table 4.5. Mole fraction of CH_4 for numerical combustion case model for 30 and 35.5mm loading heights.	56

LIST OF SYMBOLS

W_i	Net Wobbe number (MJ/m ³)
W_s	Gross Wobbe number (MJ/m ³)
H_i	Net calorific value (MJ/m ³)
H_s	Gross calorific value (MJ/m ³)
d	Relative density (kg/m ³)
Q_n	Heat input (kW)
\dot{V}_n	Volumetric rate of the gas (m ³ /h)
η	Thermal efficiency (%)
m_e	Equivalent mass (kg)
T	Temperature (K, °C)
V_c	Volume of consumed gas (m ³)
P	Pressure (Pa)
v	Specific volume (m ³ /kg)
R_u	Universal gas constant (kJ/kmole.K)
R	Constant of a specific gas (kJ/kg.K)
n	Number of moles
γ_i	Mass fraction of component i
m_i	Mass of component i (kg)
\mathcal{G}_i	Mole fraction of component i
M_i	Molecular weight of component i (g/mole)
ϕ	Fuel-to-air equivalence ratio
λ	Air-to-fuel equivalence ratio
c_p	Constant pressure heat capacity (kJ/kg.K)
c_v	Constant volume heat capacity (kJ/kg.K)
h	Enthalpy (kJ/kg, kJ/mole)
Re	Reynolds number
V	Velocity (m/s)
ρ	Density (kg/m ³)
D	Injector diameter (m)
μ	Dynamic viscosity (Pa-s)

CHAPTER 1

INTRODUCTION

Air pollution is a global hot topic and fossil fuels are widely used throughout the world. Governments take precautions and make agreements to reduce carbon emission in global scale. Reducing CO and CO₂ emission rates to an acceptable level are one of the important topics. However, there is no such an agreement for indoor air quality in global scale and indoor air pollutants can be crucial to human health.

In United States, Environmental Protection Agency ranks indoor air pollution sources that release gases or particles into the air are a primary cause of indoor air quality problems in homes and gaseous pollutants are mentioned as one of the important pollutants that increase risks of chronic health problems [1]. EPA sets national ambient air quality standards to protect both the general population and sensitive sub-populations. [2-3]. Similarly, in Europe, European Environment Agency ranks carbon monoxide and nitrogen dioxide among top six indoor air pollution sources, which can be fatal in high doses [4].

In developing countries, energy used for cooking constitutes a significant portion of the total energy requirement, while in developed countries, this is generally ignored because of its negligible contribution to the total energy. Nevertheless, considering the high usage of fossil fuels, even a small improvement in terms of performance and/or pollutant emissions will make a significant positive effect in global scale. For this cause, a study over a prototype domestic cooker top appliance which burns gas has been initiated.

Although domestic gas cooker top appliances are common, the way they work must be described. The fuel flow is controlled by the knobs, which are connected to manual valves. When the knob is turned, the fuel comes to the injector from main collector pipe. As the fuel goes out of injector, it first arises as a jet through gas burner's body and starts to entrain air from ambient. With this entrainment, a fuel/air mixture occurs. The mixture goes through the burner's ports and then it is ignited. Considering that the released heat is only controlled by fuel flow rate with changing the knob position,

it is challenging in cooker appliance design, since all the geometry during functioning is fixed. Despite this condition, the appliance must work well enough in different countries, in which different gas types are in use as fuel. A change in fuel causes a change in density, viscosity, calorific value and chemical reactions, which causes a complete change of behavior of the appliance.

To understand the appliance better and to provide a better insight, it is also important to use a numerical model. Although there are several studies in this field, the numerical investigation is so limited. There is a need to extend the studies into three dimensional processes and predict the heat transfer to the cooking vessel. To do this, a commercially available software is used in scope of this study.

In chapter 2, the studies in similar field will be described. After this, to provide a better insight, a detailed explanation of the way of how a domestic cooker top appliance work will be described and some theoretical background will be given in chapter 3. To see the performance of the appliance, some of the applied tests are described in the same chapter. Then, the preliminary results of both experimental tests and numerical modelling will be given in chapter 4. Later, the effects of changing loading height over thermal efficiency and pollutant concentrations will be given in the same chapter. Finally, the obtained information and the future work will be summarized in chapter 5.

CHAPTER 2

LITERATURE SURVEY

Burners are used widely in heating processes and their high thermal efficiency is one of the important requirements. Considering that gas cooktops, which work with natural gas (NG) or liquefied petroleum gas (LPG), are widely used in domestic cooking, even a slight improvement in thermal efficiency or reduction of pollutant emission rates will have great impacts on world's fossil fuel consumption rate. With increasing concern for air pollution, various studies with different approaches have been performed on gas cooktop burners.

2.1. Field Studies

There are different field studies, which mostly aim creating awareness on indoor air pollutants and their effects on human health.

A field study by Moschandreas [5] shows conclusive data, which are generated from 12 different homes in United States, shows differences between indoor air sampling and grab sampling, which is a frequently used method for indoor air sampling. Results show that concentrations of nitrogen oxide, nitrogen dioxide and carbon monoxide are observed to have differences in homes with gas appliances, but not in homes with electric appliances. It is noted that the kitchen is not always the zone with maximum pollutant rates, even in homes with unvented gas appliances. The results also show that, one sampling zone is not enough to specify indoor air pollution concentration and having more than one indoor zone would be a better approach [5].

Another field study remarks the indoor nitrogen dioxide exposure in Australia. The study mentions Australia's asthma occurrence as the highest in the world and claims that indoor environment has an important role. The focus of research is pointing out that there are other factors that can have an effect and links it with nitrogen dioxide exposure. It claims that source and concentration of this pollutant has not been analyzed in homes

and it has been associated with breathing problems. Most critical sources of nitrogen dioxide, which are commonly used in homes, are gas cooking appliances and gas heaters. Because of these appliances, indoor concentrations of nitrogen dioxide easily exceed outdoor levels. For this study, eighty homes were used. Nitrogen dioxide sampling was done in periodically, which makes five sampling in total and employment lasted four days. The number of gas cookers and gas heaters was noted. In addition to these, relative humidity and temperature were measured in every targeted room.

Results show that mean indoor nitrogen dioxide level for sampling period is higher than the mean outdoor nitrogen dioxide level. As it can be seen in Table 2.1, results also indicate that there were significant differences between rooms such as it is seen that higher nitrogen dioxide concentrations were measured in kitchens than the other rooms. It is also mentioned that higher nitrogen dioxide concentrations were measured in houses with gas cookers and ventilated gas heaters. Finally, it was remarked that Australia does not have an indoor guideline for nitrogen dioxide and offers to define a maximum concentration limit [6].

Table 2.1. Nitrogen dioxide levels ($\mu\text{g}/\text{m}^3$) recorded in rooms with major nitrogen dioxide sources present in the house (Source: [6])

Source	n	Bedroom		Living Room		Kitchen	
		Mean	Range	Mean	Range	Mean	Range
None	15	5.8	<0.7-15.9	7.2	<0.7-17.7	7.3	<0.7-15.6
Gas stove	15	12.1	<0.7-36.0	12.8	3.0-35.0	15.3	5.0-46.1
Gas heater	14	9.6	<0.7-24.0	13.1	4.2-34.5	14.0	5.5-50.1
Smoking	7	10.8	2.4-52.9	11.5	1.8-27.9	12.6	3.5-31.4
Multiple	29	21.3	1.8-214	27.7	4.3-219	20.5	5.0-246

A recent field study in United States aims increasing the awareness that natural gas appliances are a source of indoor air pollutants in homes. In the study, researchers investigated the cooking appliances, ventilating and heating systems in nine different homes. The natural gas cooking burner operations were designed to imitate cooking procedure. To prevent pollutant production from preparation of food, vessels which contain water were used. NO_x , NO, CO and CO_2 were measured in the kitchen and in a

room, which was far from the kitchen. Experiments included forced air units and ventilating range hoods as a part of observation to see their effects. The cooking was simulated with vessels and range hoods were activated if it was a part of test. Sampling equipment continuously monitored the concentrations of targeted pollutants.

Results mention that indoor air pollutants can be reduced to a certain level with a venting range hood or another appropriate exhaust system. Study also remarks that building standards must require venting hoods with airflow rate of at least 95 L/s [7].

2.2. Experimental and Numerical Studies

Many experimental studies have been performed over performance of gas cooktop burners.

An experimental investigation, performed by Hou et al. [8] aimed observing the effects of significant parameters, such as swirl flow, loading height, primary aeration, gas flow rate, gas supply pressure on thermal efficiency and carbon monoxide concentrations of domestic gas burners. The study especially focuses on the effects of having a swirling flame on the performance of a new burner design, which is mentioned as swirl burner. In order to have more accurate performance comparison between swirl burner and a common radial burner, only the outer ring was changed, while the remaining components were kept the same. The tests were performed with both burner types with changing other parameters which are mentioned earlier. Liquified petroleum gas was used as fuel for the tests. Effect of each parameter on thermal efficiency and carbon monoxide concentration was observed. As it can be seen in Figure 2.1, results show that port design of a burner has a significant effect on type of flow, and this affects the burner performance in terms of pollutant emission and efficiency. The swirl burner has a higher thermal efficiency and only a small amount of higher carbon monoxide level than the common radial burner. In conclusion, the study offers using the swirl burner with a circular shield, which delays the exhaust of flue gas and scattering of the flame, which helps increasing thermal efficiency [8].

In 2003, Ko and Lin [9] published a study over the effects of natural gas with different heating values over burner performance. The study mentions many parameters that would affect the burner performance, including supplying appropriate fuel-air ratio,

having a reliable and controlled ignition, stable shape and structure of flame, design of the parts and operational conditions. Although there are many studies, which are focused on design, fuel-air mixture and ignition, there are not so many researches over the effects of gas composition. Calorific value of a fuel is defined by its composition and using the same gas burner to burn natural gas with different calorific values may be hazardous because of high possibility of incomplete combustion occurrence with liftoff and flashback. Under these conditions, it is aimed to show the effects of changing gas composition on burner performance. Afterwards, propose an appropriate design or operating conditions for domestic gas cooker that burns natural gas with different calorific values. Although the study particularly focuses on gas composition, it also observes the effects of gas supply pressure, gas flow rate, primary aeration and loading height of the vessel.

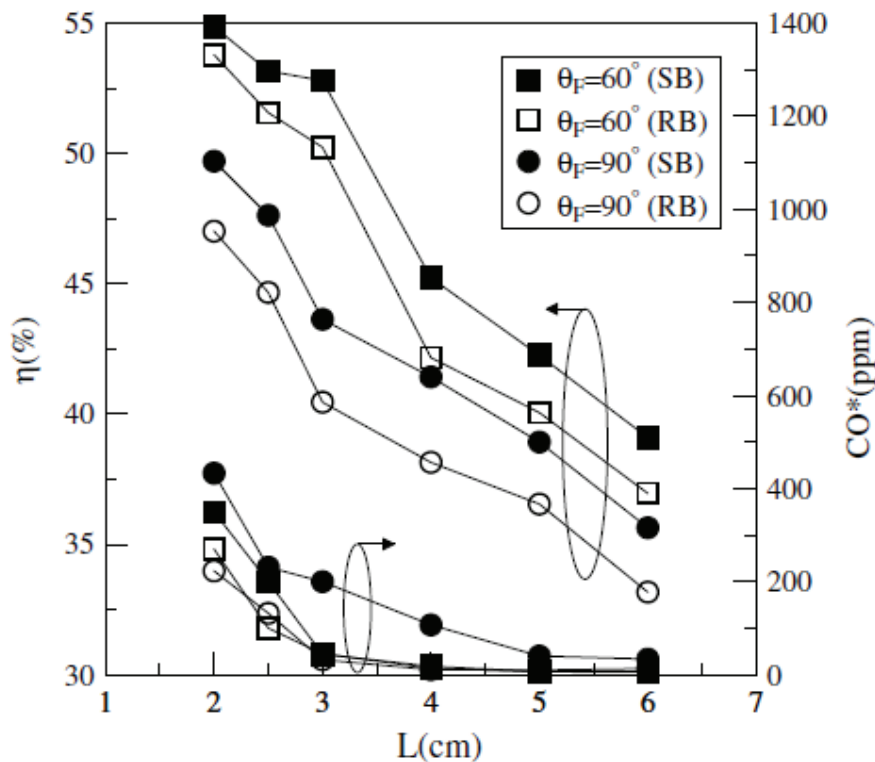


Figure 2.1. Change in CO emission and efficiency against loading height at different thermal inputs, provided by fuel regulator opening angle (Source: [8])

The experiment was operated by using natural gas with two different calorific values. The natural gas that with higher calorific value contains more combustible

products than the low calorific value natural gas. This means having higher calorific value increases the amount of needed air to achieve combustion stoichiometry and the possibility of incomplete combustion. To have a dependable conclusion tests were performed with mentioned natural gas mixtures with a various appliance. For experiments, a burner, which is mainly suitable to operate with low calorific value natural gas, was used to see the effects of changing gas composition on the thermal efficiency and pollutant emission. The pollutant concentrations and thermal efficiency from the gas cooker are measured by the sampling and analysis. In order to calculate thermal efficiency, water temperature was measured with thermocouple from the middle point of the water level.

The results show that using natural gas with higher calorific value instead of a lower calorific value gives a result of decrease in thermal efficiency. This is mainly caused by higher heat input that is provided by higher calorific value. It also causes an increase of carbon monoxide concentration, due to incomplete combustion. It is noted that, a similar result was observed in a similar study. However, in that study, the thermal input was maintained by changing the fuel flow rate instead of using different gas composition. Although using higher calorific value results in a negative way, results also say that if this type of natural gas is used with adjustment of other parameters such as primary aeration, gas flow rate, gas supply pressure, loading height, a decrease in carbon monoxide concentration and an increase in thermal efficiency is observed [9].

Another study focuses on a new burner structure design to improve thermal efficiency and emissions. The study by Sumrerng et al. [10] is based on heat-recirculation in a combustion system, which is based on the porous medium technology. Such burner for domestic use was defined as porous radiant recirculated burner. In the study, it was mentioned that conventional burners have low thermal efficiency and an improvement with this technology should be considered.

The study is mainly divided into two major topics. The first one is an application of the technology to have the exhaust gas recirculation in the typical domestic burner. The second one is an application of the technology to a swirling central flow burner. The increase in efficiency in swirl burner is basically obtained by improved heat transfer coefficient and bigger heat transfer region at the bottom of the vessel.

The focus in this study is to increase thermal efficiency with this technology, while keeping the pollutant concentrations as low as possible. For experimental setup,

burner with a capacity in a range from 5 kW to 30 kW is used. To get the exhaust gas back in the system to preheat the primary air, a pair of emitting and absorbing porous mediums are arranged.

As it can be seen in Figure 2.2, the results of experiment show that, the studied technology and structure works well to recirculate the exhaust gas. By integrating the new structure with a typical burner, thermal efficiency was increased by 12%. On the other hand, integrating the structure with the swirl burner resulted with a thermal efficiency value about 60%, which is double of typical burner. This provides a chance to reduce energy consumption 50% additionally. Moreover, the new burners also provide negligible changes in pollutant concentrations [10].

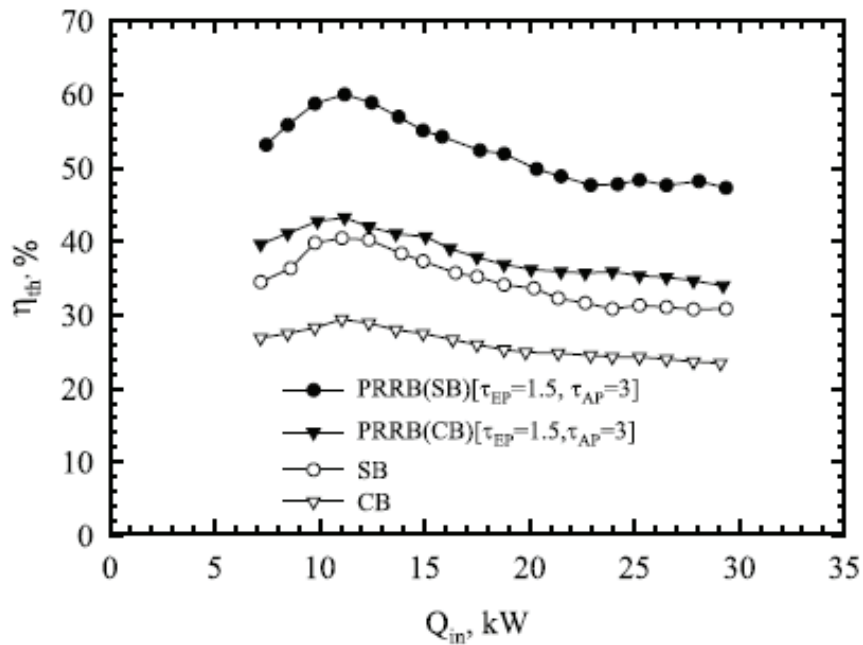


Figure 2.2. Change in thermal efficiency with varying burner power for different burner types (Source: [10])

In 2012, Boggavarapu et al. [11] published an article over domestic gas burners, which includes both experimental and numerical approach. In the study, it is pointed out that even though there are many investigations over domestic gas burners to see effects of different parameters on pollutant emissions and thermal efficiency, there are limited numerical studies, where detailed parametric studies are done. Even in the limited number of numerical studies, the relevant study to the knowledge of the author was limited to a two-dimensional analysis. This type of studies should be extended to three-dimensional

analysis to predict the heat transfer to the cooking vessel. Then with the gained knowledge from the numerical model, design changes would be proposed which would be implemented and tested experimentally. In the study, the relation of vessel size and the amount of water in it were given in the standard with flow rate of gas. As the burner starts to operate, the time is measured until when the water temperature reaches to 90 °C.

For the numerical modeling, it is pointed out that it was not applicable to simulate all the steps of experiments which were performed as mentioned earlier. That is why a steady state analysis with combustion and heat transfer was modeled. The final results were gained in two steps. First, a cold flow of the fuel was performed in the simulation without combustion reactions. Afterwards, the reactions are switched on and ignition is patched into the region. This two-step solution helps improving the convergence of the residuals. Moreover, it reduces computation time.

Based on the insights from the CFD model, design modifications were done to increase thermal efficiency as shown in Figure 2.3. With experiments, the results of the simulations were validated and an increase in thermal efficiency was obtained for both liquified petroleum gas and natural gas as fuel source [11].

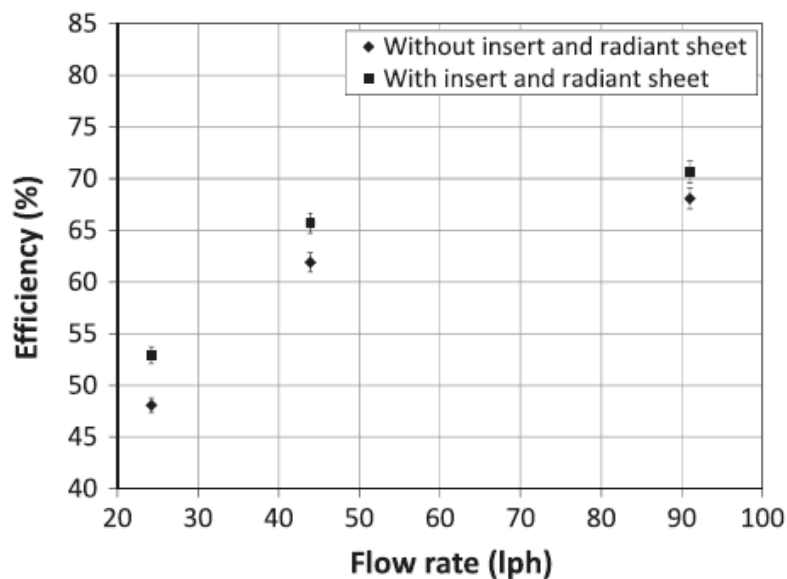


Figure 2.3. Results of thermal efficiency for different flow rates (Source: [11])

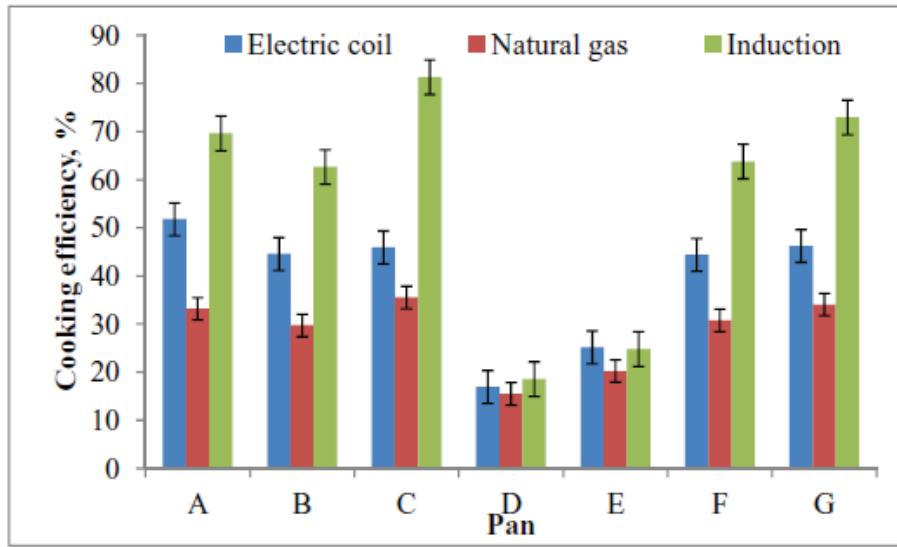
Effects of heating height was observed by Hou et al. in 2002. In study it is mentioned that number of related studies to see flame characteristics and thermal

efficiency of laminar impinging flame is very limited. Loading height of the pot is an important parameter in domestic gas cooktop design, but there are not many studies in the literature over it. In this study, observing the effects of loading height on the flame structure, temperature distribution and thermal efficiency is aimed. For this, a laminar Bunsen-type flame is used. To simulate the flame characteristics of a domestic gas cooktop, all flames in the test were in fuel rich condition. For three different heating heights, three different flame shapes were observed. Results show that temperature distribution depends on flame structure and flame structure is affected both from loading height and fuel type. An optimized loading height for the burner is gained and offered with the evaluation of results. It was also mentioned that maximum thermal efficiency was achieved when the loading height was just a little bit lower than the flame length, which means that flame tip barely has contact with loading plate [12].

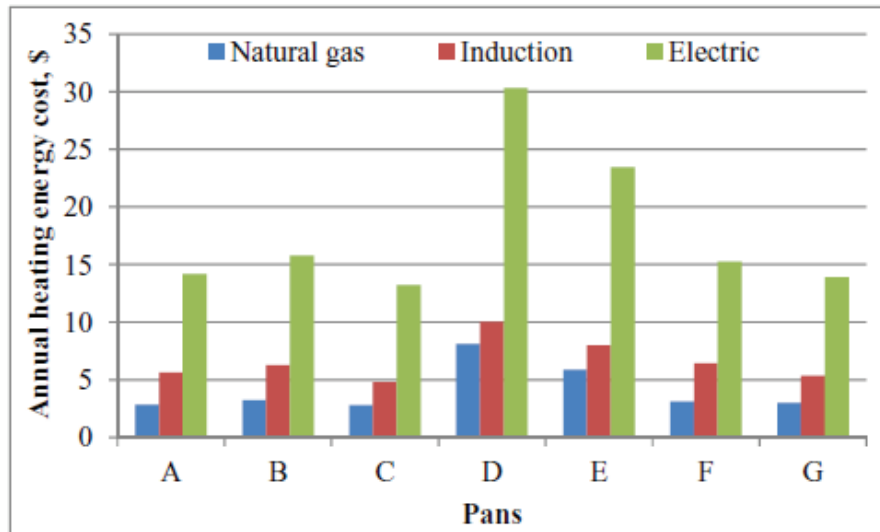
A similar study is performed by Hou and Ko to see effects of both oblique angle and loading height together. For this study, again a Bunsen fuel-rich flame was used. In experiments, same loading heights which were tested in previous study were used with 30, 60 and 90 degrees of oblique angle. As a result, it was observed that the effect of angle on flame structure is stronger for lower loading heights. This also effects temperature distribution, especially when the angle was reduced from 90 to 60 degrees. Optimum operating condition for the burner was defined by the widest high temperature zone and highest thermal efficiency value [13].

To observe cooking efficiency, Karunanithy and Shafer performed a study on various cooktops in United States. In study, it was aimed to define the energy costs of different variant of cooktops. It was mentioned that most people in United States use cooktops operating with electric coil or natural gas. However, lately, induction cooktops were gaining popularity in addition. For tests, seven different pans, which are most commonly available were used. These pans vary in thickness, weight and material, but their general size and total volume are similar. Thermocouples were used in each empty pan to measure temperature. Water at room temperature was filled in each pan and was heated until the temperature reached 90 °C. As it can be seen in Figure 2.4, results show that pan type has a huge role on cooking efficiency and each pan type has different efficiency values on each cooktop. In general, the highest efficiency values were observed in induction cooktop, where electric coil cooktop comes second, and natural gas cooktop is third. However, as heating energy costs were taken into account, it was seen that if a

person wanted to switch from electric to natural gas cooktop, the consumer would spend only 25% of the electric energy cost for cooking [14].



a)



b)

Figure 2.4. Results of a) cooking efficiency b) annual energy cost for cooker and pan types (Source: [14])

Li et al. studied effects of major design parameters of gas cooktops on thermal performance and carbon monoxide concentration. Tests were performed according to Chinese National Standard. Liquefied petroleum gas was used for the tests. Results show that Reynolds number, value of equivalence ratio, loading height and jet to jet spacing are major parameters, which have effect on both carbon monoxide concentration level and

thermal efficiency. As Reynolds number was increased, thermal efficiency decreased linearly, and carbon monoxide concentration increased to a peak value just before it started decreasing slightly. Increasing equivalence ratio value from 1.40 to 2 with 0.15 intervals was performed and it was seen that thermal efficiency first decreases to a minimum value, just before it started increasing slightly. The exact opposite situation was valid for carbon monoxide emission values. Variations of the outputs were also observed with changing loading height and jet to jet spacing. As the loading height was increased, thermal efficiency increased to a maximum value before it started decreasing slightly. On the other hand, carbon monoxide concentration kept decreasing linearly. Finally, increasing jet to jet spacing leads to an increase of thermal efficiency with carbon monoxide emission. With a developed regression model, the combined effect of these parameters was also observed. It was found that, combined effects of loading height, jet to jet spacing and equivalence ratio must be considered in thermal efficiency model. On the other hand, Reynolds number, equivalence ratio and jet to jet spacing will be more significant in carbon monoxide emission model [15].

CHAPTER 3

METHODOLOGY

To have an insight related with this study and to be able to understand the applications in domestic gas burner design, it is necessary to understand the principles of combustion. In this chapter, an introduction to combustion fundamentals will be given. Later, the domestic gas burner setup will be given, and a background information will be described. After that, a brief information of the related tests for safety requirements will be given. To have full details of the test procedures, reader must obtain the related European Standard [19,20]. Figure 3.1 shows a flow chart to summarize the experimental and numerical approach in this study.

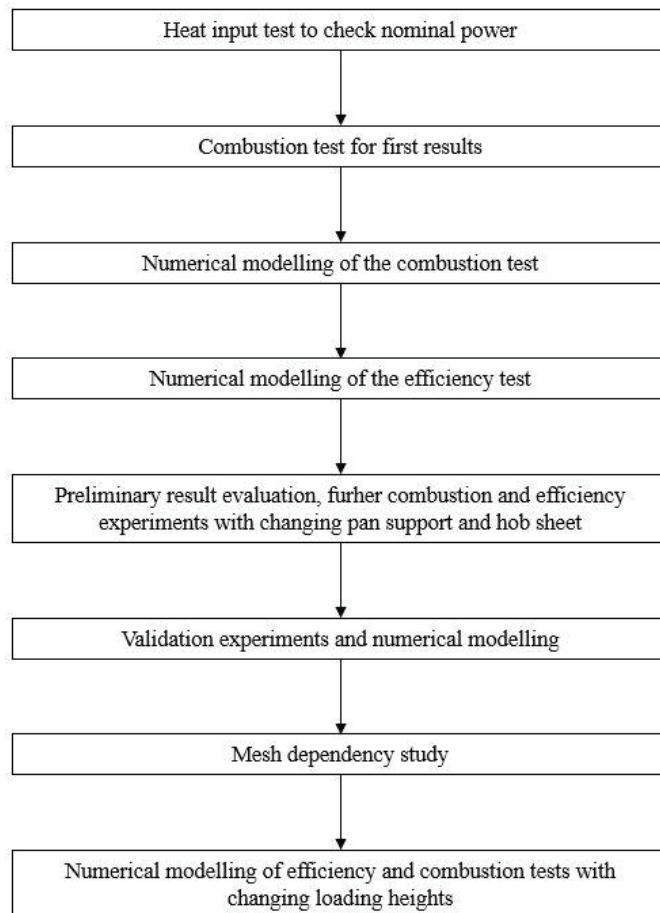


Figure 3.1. Flow chart of experimental and numerical studies

3.1. Combustion Definition

Combustion can be defined as an exothermic reaction, which releases a big amount of energy as heat. For this reaction to take place, basically there are three necessities: fuel, which contains a high amount of energy, air, which contains oxygen as oxidizer and for last, an ignitor, which starts the chemical reactions. To describe it simply,



Where F describes fuel, O describes oxidizer and P describes the products after chemical reaction. In this equation, the fuel and oxidizer are also described as reactants.

3.1.1. Flame

Flame, on the other hand, is defined as a combustion reaction with the ability to propagate through a suitable environment [16]. As you use an ignitor, fuel molecule and oxygen molecule start a reaction and they form some different molecules, which are called products. In this reaction, a big amount of energy is released, which is called heat. That energy causes other hundreds of fuel and oxidizer molecules to start reaction and a chain reaction occurs, which results in release of a big amount of energy. This is the reason of flame's propagation and the reason of why temperature of a flame is very high.

Flame types can be divided into three categories, which depend on the way that oxidizer and fuel come into contact. If combustion takes place by diffusion of oxygen into the unburnt fuel as the fuel is injected into the combustion chamber, it is called non-aerated or diffusion flame. If the required air is supplied only partially as the primary air, then the flame is said to be partially aerated, and the remaining required air (secondary air) diffuses into the hot combustion gases just as it occurs in diffusion flame [17].

3.1.1.1. Premixed Flame

If the required air for complete combustion is supplied as primary air, then the flame is called fully premixed. A simple example for a premixed flame is the flame of the Bunsen burner, in which is an air hole open, where primary air is entrained into the gas stream to form mixture. In this type of flame, a premixed flame front propagates towards the burner until it reaches its steady state position. Beyond the flame front, the unburnt products like CO and H₂ will mix with the air, which comes from ambient and post flame oxidation and radiation takes place. A model for premixed flame is shown in Figure 3.2.

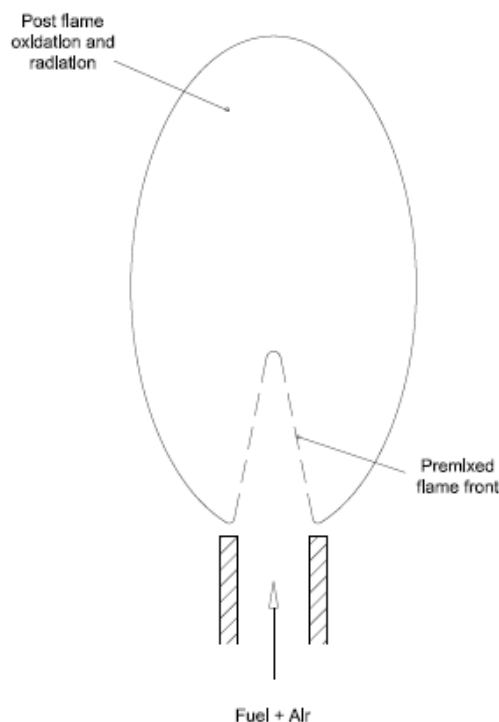


Figure 3.2. Premixed flame model (Source: [18])

Premixed flames can be analyzed in three zones:

In the preheat zone, temperature of the reactants increases to a temperature, where mixture reaches the ignition temperature. The necessary heat for this process is supplied by radiation and conduction against the direction of flow [17].

The chemical reactions occur in the reaction zone. This zone is also called as flame front. Flame front is a region with intense chemical reactions, with 0.1 mm thickness in atmospheric pressure [17]. It is visible as blue colored inner cone in hydrocarbon flames.

After the chemical reactions take place in reaction zone, fuel and air forms combustion products, such as water vapor, carbon monoxide and carbon dioxide. In addition to these, excess fuel or oxygen may remain in the same zone, depending on whether the flame is partially or fully premixed. If the flame is partially premixed, the unburnt fuel reacts with secondary air in hot, burnt gases (post flame) zone. These reactions are visible in a violet-blue color, surrounding the inner cone [17].

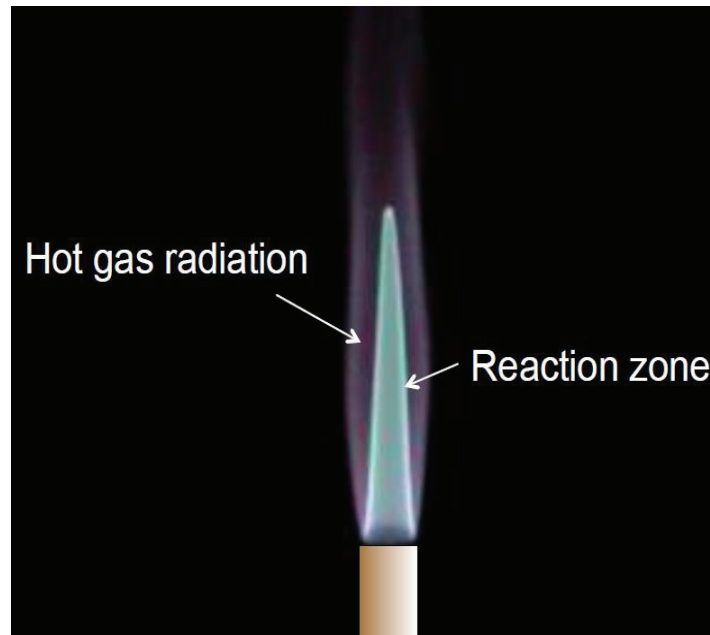


Figure 3.3. Premixed Flame Reaction and Post Flame Zones

3.1.1.2. Diffusion Flames

If the primary air is not supplied into the burner tube, neat fuel comes into the combustion chamber. In this case, combustion takes place by diffusion of oxygen from the surrounding atmosphere into the unburnt fuel. The occurring flame is defined as diffusion or non-aerated flame. Diffusion flames are not structured as well as premixed flames spatially. Because of its structure, there is no easily defined regions. The reactions only take place at the surface of the flame, where the fuel meets oxygen in proper concentration. Therefore, a flame cone does not occur as it does in premixed flames. It is only accepted that there is a thin region where the fuel/oxygen ratio is stoichiometric.

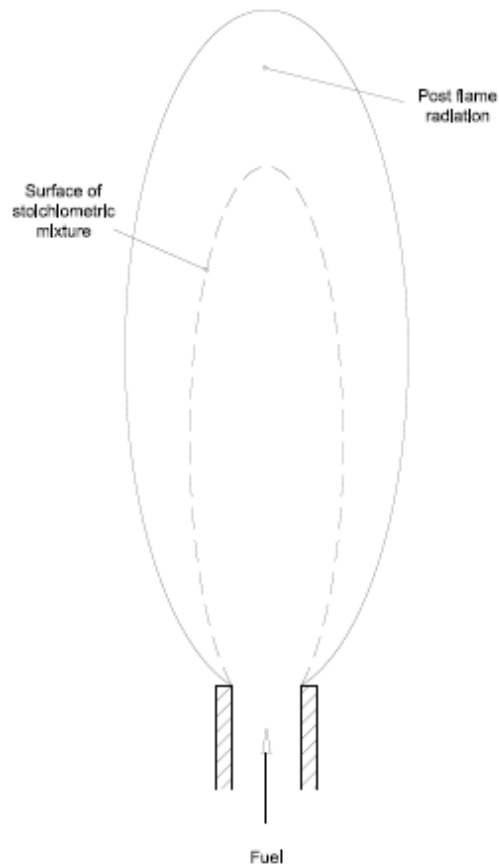


Figure 3.4. Diffusion Flame Model (Source: [18])

3.1.2. Fuel

Fuel can be defined as a source of energy, in which energy is stored in molecular structure. To consider a matter as a fuel, it should have high energy content, high heat release in combustion reaction, good thermal stability for storage, low volatility and non-toxicity.

Fuels can be categorized as solid, liquid and gaseous fuels. Although liquid fuels are used in much bigger scale in most of the combustion systems for their big energy quantities and safety of handling, gaseous fuels have the least difficulty of mixing with air and distributing homogeneously to environment.

Pure hydrocarbon fuels contain two elements, which are hydrogen and carbon. Among these, the fuels that contain four carbon atoms maximum in a molecule are gaseous, where the fuels with twenty or more carbon atoms in a molecule are solid and

those that are in between are fluid. As it will be mentioned again later in this chapter, for domestic gas cooking appliances, the range of available fuel types lie mainly within gaseous hydrocarbon fuels, which are mentioned in related European Norm as reference gases [19]. The composition of the used fuel varies, depending on the region. In scope of this study, methane will be used as fuel since it is extensively used for gas cooking appliances.

3.1.3. Flammability

For combustion to take place, fuel and air is needed. However, to have these reactants go into a reaction, there are limits. These limits define the flammability of the fuel-air mixture.

If fuel is added to air, there will be a point, where the mixture just turns into flammable. This percentage of fuel gas limit is called fuel-lean or lower flammable limit. If fuel gas will be kept added, there will be another point reached, where the mixture will not burn anymore, lacking enough oxygen. This percentage of fuel gas limit is called fuel-rich or upper flammable limit. For methane, flammability lower and upper flammability limits are given as 0.46 and 1.64, respectively in terms of fuel to air equivalence ratio [16].

3.1.4. Minimum Ignition Energy

Even if a fuel/air mixture is in flammability limits, an amount of energy is still needed to initiate the chemical reactions. This energy is called activation or ignition energy. The minimum ignition energy depends on the mixture composition, pressure, temperature and the used ignition method.

If the fuel/air mixture is raised to a high enough temperature, a point is reached at which ignition occurs spontaneously. This type of ignition is called self-ignition. The criteria for this kind of ignition is related to the net rate of heat transfer. If the heat loss is less than the heat production rate due to the chemical reactions, then ignition will take place.

If the activation energy is supplied by an external source, the type of ignition is called point ignition, in which a flame develops close to the ignition source and propagates through the reactant volume. The most practical sources for this ignition are pilot flame and electric spark.

3.1.5. Laminar Flame Speed

Burning velocity can be described as “*the velocity normal to the flame front, relative to the unburnt gas, at which an infinite one-dimensional flame propagates through the unburnt gas mixture*”. It is also called as laminar flame speed. Burning velocity is affected by the pressure, flame temperature and mixture composition. It is mostly dependent on mixture composition. In flammability limits, the velocity is almost zero and it raises to its maximum value near the stoichiometry point [16]. It is also affected by gas properties such as diffusion coefficient, viscosity and thermal conductivity [17].

In CFD, the reactant stream has one composition in fully premixed combustion model, and laminar flame speed is approximately constant throughout domain. However, in partially premixed flames, it is not the same, since the reactant composition changes. For this reason, it is usually measured by experiments.

3.2. Experimental Setup

Since gas appliance manufacturers in Europe get certification for their appliances according to the relevant European Standards, the tests for this study were performed according to the requirements of DIN EN 30-1-1:2013 and DIN EN 30-2-1:2015, which include safety and energy requirements respectively for domestic cooking appliances burning gas. In this study, heat input, combustion and efficiency tests were performed.

3.2.1. Background Information

To understand the test procedures, which will be given in the next topics, it is important to have a brief knowledge related with domestic gas cooktop burners. For this study, a cooktop product, which is still in the development process, has been used.

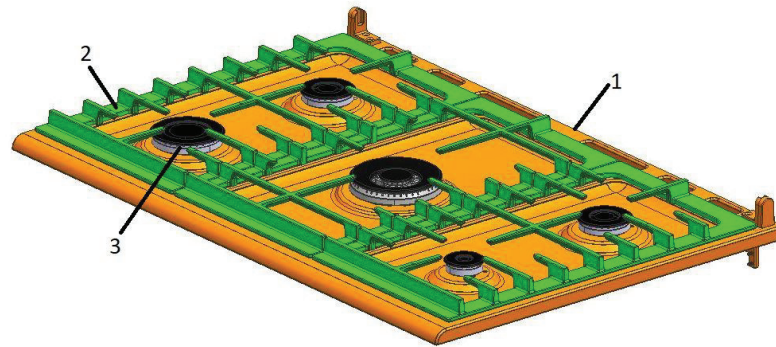


Figure 3.5. Cooktop model

In Figure 3.5., a model of the cooktop with related parts can be seen, where 1 describes hob sheet, which carries the other parts on top of it, 2 describes pan support and 3 describes burner. For different applications, power and type of the burners and configurations can vary, depending on the demand. An example of this is shown in Figure 3.6.



Figure 3.6. An example of configuration

Where burner number 1 is named as auxiliary burner, number 2 is named as semi-rapid / normal burner, number 3 is named as rapid burner and number 4 is named as wok burner. Usually, if each burner has similar concept, semi-rapid burner has the highest efficiency, comparing with rapid and wok burners. Auxiliary burner is out of scope in this term, since it is not included in to efficiency test.

To give example to burner types, in diffusion mixed burners, the fuel and oxidizer are separated and unmixed before combustion. Combustion takes place during the mixture process, when the fuel/air mixture is in flammability range. In premixed burners, the fuel and air are mixed completely before combustion takes place. The flame of these burners is usually shorter but more intense, compared to diffusion flames. Because of the flame structure, premixed burners can produce high temperature regions in the flame, which leads to non-uniform heating of the load [18].

In this study, a partially premixed burner will be investigated and hereafter will be named as “domestic gas burner”. A cross-section of the setup is shown in Figure 3.7.

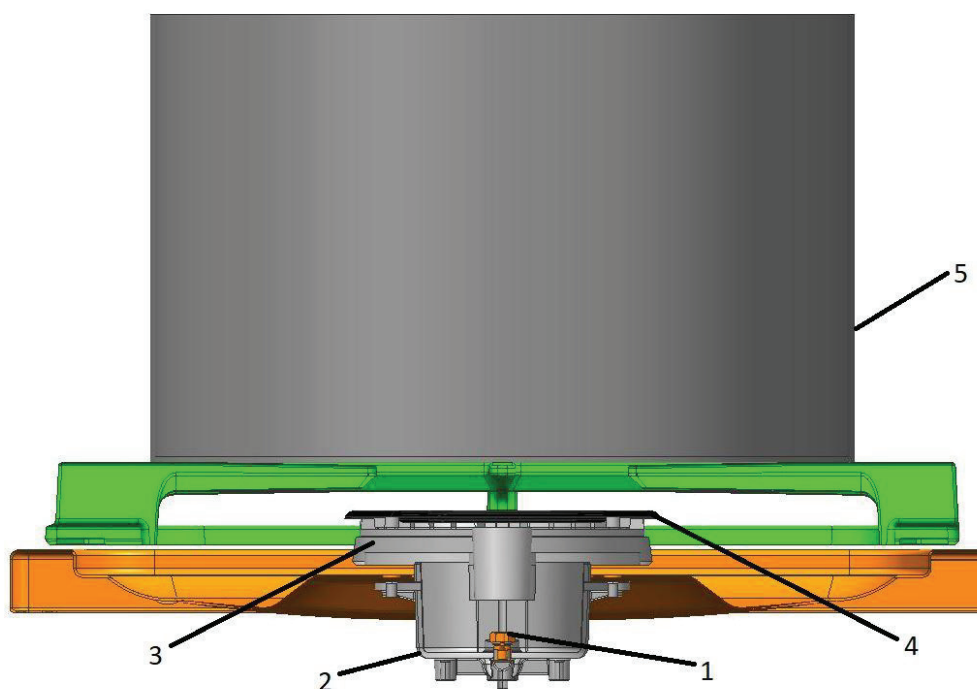


Figure 3.7. Section of a cooktop burner

Where 1 refers to injector, 2 refers to burner body, 3 refers to flame spreader, 4 refers to burner lid and 5 refers to cooking pot as load.

In this setup, when the gas supply valve is turned on, the fuel gas enters the gas supply pipe. Then the fuel reaches to the injector nozzle, which is positioned on the bottom of the injector holder body along vertical axis. When the fuel comes out of the injector outlet, it causes an entrainment force of the jet due to the pressure difference between the atmosphere and fuel jet. With this force, fuel entrains primary air, and this creates a fuel rich mixture. It is assumed that through injector holder body, mixing of the fuel/air mixture is complete due to turbulence, which is caused by high velocity of the fuel jet. As the mixture rises, inside the flame spreader, it reaches to the lid of the burner and distributes through the ports of the flame spreader. For the mixture to be able to exit uniformly through the ports, a small increase in pressure is necessary to handle the resistance of the ports. This uniformity is obtained by the decrease in velocity, which is caused by an expansion within the burner head. Then the mixture exits through the ports and feeds the flame at the outlet of the ports. Due to the mixture characteristic of this setup, the type of this domestic gas burner is called as partially premixed burner, which works in atmospheric conditions. Naming the type of the domestic gas burner as partially premixed burner is important to be consistent with the flame terminology.

3.2.2. Tests

Since the requirements depend on the type of appliance and the fuel, appliances are categorized according to the gases and pressures for which they are designed. Same categorization is valid for the gas types. The categories for gas types are defined as families, which can be divided into sub-groups according to the Wobbe number. The gases mainly used in Europe are given below in Table 3.1.

Table 3.1. Characteristics of the reference test gases (Source: [19])

	Volume Composition (%)	W_i (MJ/m ³)	H_i (MJ/m ³)	W_s (MJ/m ³)	H_s (MJ/m ³)	d (kg/m ³)
G20	CH ₄ =100	45,67	34,02	50,72	37,78	0,555
G30	n-C ₄ H ₁₀ =50 i-C ₄ H ₁₀ =50	80,58	116,09	87,33	125,81	2,075

Where W_i refers to net Wobbe number, H_i is the net calorific value, W_s is the gross Wobbe number, H_s is the gross calorific value and d is the relative density.

Relative density is ratio of the masses of equal volumes of dry gas and dry air under same conditions of temperature and pressure, which are given as 15°C or 0°C and 1013,25 mbar, respectively [19].

Wobbe number is the ratio between the calorific value of a gas per unit volume and the square root of its relative density under the same reference conditions. The Wobbe number can be defined as gross or net, depending on whether caloric value is gross or net.

$$W_s = \frac{H_s}{\sqrt{d}} \quad (3.2)$$

Calorific value of a gas refers to the amount of heat released from the gas molecule per unit volume or unit mass by combustion. The difference between gross calorific value and net calorific value is related with the energy released by water during combustion process. If the water vapor, which is produced by combustion process, condenses, it releases an additional heat. In net calorific value, the water remains gaseous. That is why gross calorific value is also called higher heating value, while net calorific value is called lower heating value.

3.2.2.1. Heat Input

Heat input test is performed to declare the nominal power of the burner. Most frequently, domestic gas burner suppliers offer an injector hole diameter to be used with a specific reference gas to provide the power which is declared by the supplier. This still needs to be tested by the domestic appliance manufacturers to declare that they meet the requirements of the related norms. For this test according to the related standard, an aluminum pot, which has 220-millimeter inner diameter, is filled with 2 kilograms of water. The dimensions of pot and the amount of water is constant for this test for all power values of cooktop burner. The water simulates the food in customer use. First the burner

operates at designated nominal gas inlet pressure for 10 minutes to preheat the injector. This ensures to have the injector in a stable form after its expansion with rising temperature. As flow rate changes with the effect of injector diameter change after its expansion, gas inlet pressure is adjusted accordingly to keep it at its nominal value. The nominal heat input declared by the manufacturer is given in the expression below:

$$Q_n = 0.278\dot{V}_n H_s \quad (3.3)$$

Where Q_n is the power expressed in kilowatts, \dot{V}_n is the volumetric rate of the reference gas in cubic meter per hour and H_s is gross calorific value of the reference gas, given in megajoules per cubic meter. The flow rate is measured by a gas meter, which has 1.2% error tolerance.

Since static pressure at injector is proportional to volume rate, it can be said that gas inlet pressure is decisive in heat input value. The static pressure values of reference gases G20 and G30 are given below in Table 3.2:

Table 3.2. Test pressures for reference gases: 2H(G20) and 3B/P (G30) (Source: [19])

Test Gas	Pressure (mbar)		
	Minimum	Nominal	Maximum
G20	17	20	25
G30	20	29	35

Where the pressure values correspond to the gas distributed nationally or locally.

3.2.2.2. Combustion Test

Combustion test is done to see the burner's performance in terms of pollutant concentrations. For the appliances, combustion performance requirements are linked to the volumetric concentration of CO in the air- and water-free products of combustion.

Since the emission of NO_x is very low for these appliances, it is negligible according to the related standard [19]. After installation of the appliance, each of the burners must be adjusted to their nominal heat input. Mainly, the concept of the test procedure is similar to heat input test. However, the used pot diameter changes according to the nominal power of the burner. If the nominal power of the burner is lower than 4.2 kW, a pot with 220-millimeter inner diameter must be used for the test, with 2 kg of water inside. If the nominal power is higher than 4.2 kW, the diameter must be 300 millimeters, with 3 kg of water inside for the test. Before the test starts, a hood, which surrounds the pot is placed on. The hood is used to get sample from flue gas of the burner to measure the concentration of CO and CO₂. The design of the hood also allows to discharge the water vapor, which occurs due to the boiling of water inside the pot, from a different channel, so that sample for pollutant measurements can be water free.

There are 6 different test procedures, which depend on the burner type in operation and the used gas. An overview of the most common tests is given in Table 3.3:

Table 3.3. Test conditions and maximum limit of CO concentration (Source: [19])

Test No.	Burner in Operation	Used Gas	Position of Knob	Maximum CO Concentration % / Vol
1	Each burner individually	Each reference gas	Full on	0,10
2	Each burner individually	Each reference gas	Position corresponding to half of nominal heat input	0,15
3	Each burner individually	Limit gas for incomplete combustion	Full on	0,15

Where position of knob decides how much power to apply during the test, while CO concentrations are in molar/volumetric scale.

For almost each gas family, there is a different gas composition as reference gas for the tests to perform with. However, performing the tests with reference gas is not enough in scope of combustion test, as this test represents the both environmental and health safety with performance of the burner in pollutant emission scale. To see the

possible worst-case scenario, there is a defined gas for each gas family as limit gas. The limit gases mostly have a different composition than the reference gas of the same gas family. The difference is provided by addition of different compounds and molecules into the fuel content. The background of introducing limit gas is based on distribution of fuel from a national pipeline. As it is needed, the gas distribution line sometimes needs to be pressurized, to provide fuel to people in the pressure range given earlier in Table 3.2. To provide this pressure, additive gases are used and of course, due to this addition, the mixture and calorific value of the fuel changes. The rate of these additives inside the fuel is measured to define a gas composition, which creates the limit gas content. To summarize, it is convenient to call limit gases as “*the test gases, which represents the extreme variations in characteristics of the gases for which the appliances have been designed*” [19]. Another reason would be to increase the calorific value of the gas in winter season as it is done in some regions. An example can be given for methane, which is called G20 as reference gas. The limit gas of G20 is called G21, which includes %87 methane and %13 propane by volume. Since the appliances are not designed mainly for the limit gases and the additives have bad influence on combustion process, the success criteria for the tests with these gases are higher than the tests with reference gases.

For the combustion product sampling, Ultramat 23, a commercial sample analyzer was used. This analyzer’s measurement principle is based on absorption of bands of infrared radiation. The analyzer gets the combustion product samples and in condensation chamber, it condenses the water vapor to give dry concentrations. Infrared radiation passes through the sample chamber and its intensity decreases, depending on the concentration of the measured component. The radiated energy is absorbed by the combustion products and detector inside the analyzer detects the concentration of samples by measuring how much energy is radiated by them. Since the wavelength of each component is different, analyzer is able to measure concentrations separately. On top of measuring oxygen concentration, the analyzer is able to measure two additional defined components at the same time. The measuring ranges vary, depending on the defined component couple. For CO and CO₂ coupling, the measuring range is 0-0.5% and 0-10% respectively, with 3% measuring tolerance.

3.2.2.3. Efficiency Test

Efficiency tests are performed to declare the thermal efficiency of the gas cooking appliances according to EN 30-2-1. If the nominal heat input of the burner is lower than 1.16 kW, the test is not applicable. The efficiency of each single burner under test must be more than 52% to be successful. As an example, the pan diameter and mass of water depending on the burner nominal heat input are given below in the Table 3.4 for some cases:

Table 3.4. Test conditions for different nominal heat input values (Source: [20])

Nominal Heat Input of the Burner (kW)	Internal Diameter of the Test Pan (mm)	Mass of Water to be Used (kg)
1.99 – 2.36	260	6.1
2.37 – 4.2	260 with an adjustment of the heat input of the burner to $2.36 \text{ kW} \pm 2\%$	6.1
Greater than 4.2	300 with an adjustment of the heat input of the burner to $4.2 \text{ kW} \pm 2\%$	9.4

Test procedure defines a preheating process. The burner is operated with 220 mm diameter pan, containing 3.7 kg of water for 10 minutes at its nominal heat input or at the adjusted input according to conditions mentioned in the Table 3.4. After preheating, a suitable test pan according to nominal heat input of the burner will be placed over the burner, with required amount of water inside. The initial temperature of the water must be 20 ± 1 °C and the temperature at the time of extinction of the burner must be 90 ± 1 °C. This measurement of water temperature is done from the center of the water volume, with a thermocouple which has measurement uncertainty less than 0.1 °C. Similarly, the mass measurement has an uncertainty of 0.1%. The efficiency of the burner is calculated as below:

$$\eta = \frac{4.186 \times 10^{-3} m_e (T_2 - T_1)}{V_c H_s} \times 100 \quad (3.4)$$

where η is thermal efficiency of the burner in percentage, m_e equivalent mass of the pan filled with water according to instructions, T_2 is the final temperature of the water at which the burner extinguishes, T_1 is the initial temperature of the water, V_c is the volume of dry gas consumed and H_s is the gross calorific value of the gas. In this equation, m_e is defined as:

$$m_e = m_{water} + 0.213 x m_{pot} \quad (3.5)$$

It should be noted that, efficiency test is performed to measure the amount of heat that is transferred to the pot from the amount of released heat from combustion reaction. To clarify, thermal efficiency can be expressed as:

$$\text{Thermal Efficiency} = \frac{\text{Heat transferred to pot}}{\text{Heat input}} \quad (3.6)$$

$$\frac{\text{Heat transferred to pot}}{\text{Heat input}} = \frac{\text{Heat output}}{\text{Heat input}} \times \frac{\text{Heat transferred to pot}}{\text{Heat output}} \quad (3.7)$$

where ratio of heat output to heat input defines burning efficiency and ratio of heat transferred to pot to heat output defines heat transfer efficiency.

3.3. Numerical Background

In literature, even if there are many studies over the effects of different parameters on thermal efficiency or pollutant emission, there are not many numerical studies over domestic cooktop burners. In this study, it is aimed to perform both experimental and numerical studies to gain an insight over the flame characteristic of domestic cooktop burners. Boggavarapu et al. published a study which includes both experimental and numerical approach for thermal efficiency analysis [11]. However, changing parameters may also affect pollutant emission and in this study, this will also be considered. In previous topics, experimental background and an overview were given. However, it is also important to understand the physics as much as the test requirements to be able to gain an insight.

3.3.1. Ideal Gas and Conservation of Mass

Since state of a gas substance depends on pressure, temperature and specific volume, most state equations of a substance are complicated. That is why ideal gas assumption is convenient widely used in most of the computational analysis of related field [16]. The ideal gas equation is given below:

$$Pv = R_u T \quad (3.8)$$

where P is pressure, v is specific volume, R_u is the universal gas constant, which is equal to 8.314 kJ/(kmole.K) and ν is the molar specific volume. If we divide this equation by the molecular weight, M , the equation of the state on a unit mass scale can be written as:

$$P\nu = RT \quad (3.9)$$

where R is a constant of a specific gas and ν is specific volume. This equation of state can also be written in terms of total volume as:

$$PV = nR_u T \quad (3.10)$$

$$PV = mRT \quad (3.11)$$

where n is number of moles and m is the mass of the gas.

The conservation of mass principle is one of the fundamentals of engineering. It basically describes that the total mass of a mixture of species, which exist in either reactant or product state, remains constant. For a mixture of s number total chemical species, a mass fraction γ_i for each i component species can be written as:

$$\gamma_i = \frac{m_i}{m} \quad \text{and} \quad \sum_{i=1}^s \gamma_i = 1 \quad (3.12)$$

and the total mass m is equal to:

$$m = \sum_{i=1}^s m_i \quad (3.13)$$

Even if the total mass of a combustion process may remain constant, concentration of species changes during reaction. Therefore, it is more convenient to describe species in a molar scale. For a mixture of s number of total species, a mole fraction ϑ_i for each species is:

$$\vartheta_i = \frac{n_i}{n_t} \text{ and } \sum_{i=1}^s \vartheta_i = 1 \quad (3.14)$$

Alternatively, total number of mole and mass of each species can be shown as:

$$n_t = \sum_{i=1}^s n_i \text{ and } m_i = n_i M_i \quad (3.15)$$

where M_i is the molecular weight of species i .

3.3.2. Combustion Stoichiometry and Equivalence Ratio

As it is described earlier, combustion process occurs when a fuel burns with the oxidizer, air. For this reaction to take place, the rate of air that is used with the rate of fuel is important. The term stoichiometry must be introduced at this point. The aim of stoichiometry is to determine how much air is needed to completely oxidize the fuel to products carbon dioxide and water vapor. To give an example from the combustion process of methane as fuel and air as oxidizer, the complete combustion reaction can be written as:



This equation shows the breakdown of bonds between elements, which form the molecules of oxygen and methane and then forming new molecules of carbon dioxide and water. This complete combustion process assumes the chemistry would be unchanged by the inert nitrogen.

The coefficients of molecules in this equation describes stoichiometric proportions of fuel and air (reactants), with no excess fuel or oxidizer. When all species

which take part in this reaction are treated as ideal gases, the coefficients in the reaction can also be considered as volumetric proportions as well as moles of the specie, since at a constant temperature and pressure of a mole of an ideal gas occupies the same volume.

The stoichiometric air-fuel ratio by mass for this equation can be written as:

$$AFR_m = \frac{m_{air}}{m_{methane}} = \frac{\vartheta_{O_2}M_{O_2} + \vartheta_{N_2}M_{N_2}}{\vartheta_{CH_4}M_{CH_4}} \quad (3.17)$$

$$AFR_m = \frac{2 \times 32 + (2 \times 3.76) \times 28}{16} = 17.16 \frac{kg \text{ air}}{kg \text{ CH}_4}$$

which describes that for 1 kilograms of methane, 17.16 kilograms of air is needed for complete combustion to take place. The stoichiometric air-fuel ratio can also be defined by volume (mole):

$$AFR_v = \frac{\vartheta_{O_2} + \vartheta_{N_2}}{\vartheta_{CH_4}} = \frac{2(1 + 3.76)}{1} = 9.52 \frac{mole \text{ air}}{mole \text{ CH}_4} \quad (3.18)$$

which describes that for 1 mole of methane, 9.52 moles of air is needed for complete combustion.

In general, when fuel and oxidizer start a reaction, the proportions of reactants are not in the exact amounts which provide a complete combustion. In this case, lean and rich mixtures must be introduced.

Lean mixture describes that there is an excess amount of oxidizer in the mixture comparing to stoichiometric proportions. Similarly, rich mixture describes that there is an excess amount of fuel in the mixture. It is possible to have a complete combustion with a lean mixture, where an excess oxygen appears on the product side of the equation. However, it is impossible for rich mixture. These deviations from the stoichiometric proportion can be described with a term named equivalence ratio.

Equivalence ratio is defined as the ratio of fuel/air that is available to that required for the stoichiometric quantity. It can be shown in two ways:

$$\phi = \frac{\left(\frac{Fuel}{Air}\right)_{actual}}{\left(\frac{Fuel}{Air}\right)_{stoichiometry}} \quad (3.19)$$

where ϕ describes fuel to air equivalence ratio.

$$\lambda = \frac{\left(\frac{Air}{Fuel}\right)_{actual}}{\left(\frac{Air}{Fuel}\right)_{stoichiometry}} \quad (3.20)$$

where λ describes air to fuel equivalence ratio. If $\lambda < 1$, it means that the amount of air is not enough for complete combustion and the mixture is called air-lean or fuel-rich. If $\lambda > 1$, then the mixture is called air-rich or fuel-lean. These definitions are in the opposite way for ϕ .

3.3.3. Enthalpy and Enthalpy of Formation

The specific heat is the amount of heat that is needed to raise the temperature of a unit mass of substance by one degree. Each gas has a heat capacity, which can be described in two ways. These are heat capacity when heat is added at constant pressure, c_p or heat capacity when heat is added at constant volume, c_v .

Enthalpy is the total heat content of a system. Since the enthalpy of an ideal gas is a function of the temperature only, the specific heat at constant pressure can be given as:

$$c_p = \left(\frac{dh}{dT}\right), \quad dh = c_p dT \quad (3.21)$$

where h refers to enthalpy. In a combustion process, heat capacity of species changes due to high temperature changes. However, this is not the only parameter that affects the enthalpy of species in combustion. Since there is a chemical reaction, some species disappear as reactants and new molecules appear as products in the system and an amount of heat is released. That is why enthalpy of formation must be introduced.

In combustion, enthalpy of specie i can be defined as:

$$h_i = \Delta H_{f,i}^0 + \int_{T_0}^T c_{p,i} dT \quad (3.22)$$

where $\Delta H_{f,i}^0$ refers to enthalpy of formation at temperature T_0 and $\int_{T_0}^T c_{p,i} dT$ refers to sensible enthalpy. This equation tells that the enthalpy of species consists two type of enthalpy: the enthalpy that is needed to create a specie at temperature T_0 and the enthalpy that is needed to get the specie from temperature T_0 to temperature T . The information of enthalpy of formation for temperature T_0 is given only for temperature 0 K or 298.15 K. All elements in their standard states like O_2 , N_2 or H_2 have a standard enthalpy of formation zero. Because there is no change in their formation.

The enthalpy can also be described as molar enthalpy. The molar enthalpy can be shown as:

$$h_i^m = h_i M_i = \Delta H_{f,i}^0 M_i + \int_{T_0}^T c_{p,i} M_i dT \quad (3.23)$$

where h_i^m describes the molar enthalpy of specie i and $\Delta H_{f,i}^0 M_i$ is the enthalpy of formation at temperature T_0 in molar quantity, can also be written as $\Delta H_{f,i}^{0,m}$. Similar definition can be done for $c_{p,i} M_i$ as $c_{p,i}^m$ as molar heat capacity.

Earlier, mass fraction and mole fraction were defined. If these two definitions are linked,

$$\gamma_i = \frac{n_i M_i}{n M_{mean}} = \frac{M_i}{M_{mean}} \vartheta_i \quad (3.24)$$

where M_{mean} is mean atomic weight. Mean atomic weight is not constant because it has a different value in fresh gases and burnt gases. It can be found as:

$$\sum \gamma_i = 1 = \frac{\sum \vartheta_i M_i}{M_{mean}}, M_{mean} = \sum_1^s \vartheta_i M_i \quad (3.25)$$

For the mixture, the definition of mass enthalpy can be done as:

$$h = \sum_{i=1}^s h_i \gamma_i = \sum_1^s \Delta H_{f,i}^0 \gamma_i + \int_{T_0}^T \left(\sum c_{p,i} \gamma_i \right) dT \quad (3.26)$$

Molar enthalpy can be defined similarly:

$$h^m = \sum_{i=1}^s h_i^m \vartheta_i = \sum \Delta H_{f,i}^{0,m} \vartheta_i + \int_{T_0}^T c_p^m dT \quad (3.27)$$

In Table 3.5. some examples are given for mass and molar enthalpy of formations.

Table 3.5. Enthalpy of formation (mass and molar) for some species at 298 K and 1 bar
(Source: [16])

Specie	Molecular Weight, M (kg/mole)	Mass Enthalpy of Formation, $\Delta H_{f,i}^0$ (kJ/kg)	Molar Enthalpy of Formation, $\Delta H_{f,i}^{0,m}$ (kJ/mole)
CH ₄	0.016	-4675	-74.8
H ₂ O (vapor)	0.018	-13433	-241.8
CO ₂	0.044	-8943	-393.5
O ₂	0.032	0	0
N ₂	0.002	0	0

3.3.4. Adiabatic Flame Temperature

If a complete combustion process takes place without any heat loss, then all the energy, which is released from the reactants during the chemical reaction, is transferred to products. The temperature at which the products reach in this kind of reaction is called adiabatic flame temperature. This is the maximum temperature that products can reach, assuming the combustion process takes place in stoichiometric conditions and at constant pressure, and there is no shaft work.

For the calculation of adiabatic flame temperature, process can be shown as in Figure 3.8:

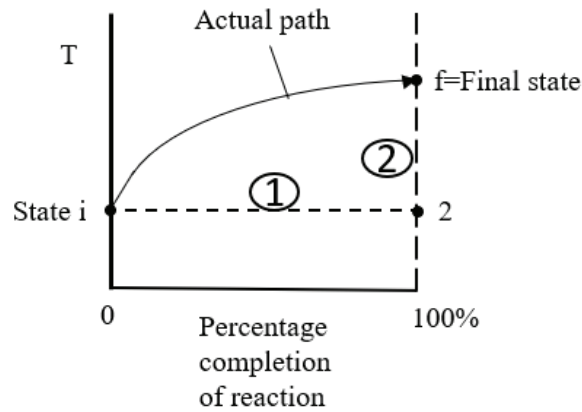


Figure 3.8. Schematic of adiabatic flame temperature (Source: [21])

As shown in the Figure 3.8, the process can be divided into two sub processes. The first process is the reaction at constant temperature and pressure. To do this, the heat must be taken away from the process. If we assume that the heat taken away from the process is Q_m :

$$h_2 - h_i = -Q_m = \sum \Delta H_{f,i}^{0,m} \vartheta_i \quad (3.28)$$

Then in second process, if we include the heat back to the process:

$$h_f - h_2 = Q_m \quad (3.29)$$

If the specific heat values are assumed constant, using an approximately average value, the equation can be shown as:

$$c_{p,avg}(T_f - T_2) = Q_m \quad (3.30)$$

The temperature change can be defined as:

$$(T_f - T_2) = \frac{\sum \Delta H_{f,i}^{0,m} \vartheta_i}{c_{p,avg}} \quad (3.31)$$

Global reaction can be shown as:



where $\vartheta'_i M_i$ defines the reactants in the reaction at temperature $T_2 = T_i$ and $\vartheta''_i M_i$ defines the products in the reaction at temperature T_f . For an adiabatic process,

$$\sum_1^s \vartheta''_i \int_{T_i}^{T_f} c_{p,i}^m dT = \sum_1^s (\vartheta'_i - \vartheta''_i) \Delta H_{f,i}^{0,m} \quad (3.33)$$

For enthalpy of formation side:

$$\sum_1^s (\vartheta'_i - \vartheta''_i) \Delta H_{f,i}^{0,m} = \Delta H_{f,CH_4}^{0,m} - \Delta H_{f,CO_2}^{0,m} - 2\Delta H_{f,H_2O}^{0,m} \quad (3.34)$$

$$\sum_1^s (\vartheta'_i - \vartheta''_i) \Delta H_{f,i}^{0,m} = -74.8 - (-393.5 - 2 \times 241.8) = 802 \text{ kJ}$$

which means burning one mole of CH₄ releases 802 kJ heat.

There are different ways to find adiabatic flame temperature. One of them is assuming an average value of heat capacities for species, as mentioned before. This will give an approximate solution. If heat capacities of gases at 1000 K temperature are used as representative:

Table 3.6. Heat capacities of gases at 1000 K and 1 bar

Specie	Heat Capacity, c_p (J/moleK)
H ₂ O (vapor)	41.2
CO ₂	54.4
N ₂	32.6

If we use these values for calculation of adiabatic flame temperature in equation 3.33:

$$802000 = (1 \times 54.4 + 2 \times 41.2 + 2 \times 3.76 \times 32.6)(T_f - T_i)$$

$$(T_f - T_i) = 2099.5 \text{ K}$$

Assuming that the initial temperature was 298.15 K, final temperature for methane flame can be found as:

$$T_f = 2397.65 \text{ K}$$

3.3.5. Numerical Modeling

After experimental study had been performed for the target appliance, preparations of numerical study were started. For numerical modelling, Ansys Fluent was used. The aim of the numerical analysis is not only modelling the heat transfer to pot, but also observing the flow and chemical reactions which take place around the domestic gas burner. For creating the domain, the 3D CAD data of the cooktop was used. 3D analysis is necessary to model geometry of burner and pot, to be able to compare with experimental studies properly. In a 2D analysis, burner and flame could not be modeled in space. The unnecessary zones are removed from the data. The flow field and the pot as the solid part are taken into consideration to create a solid/fluid mixed domain. Since the interest of this study is the rapid burner with 3 kW nominal power, only the burner and its environment were modelled.

Considering the computational costs, some simplifications and assumptions must be considered. For both simulating the combustion and efficiency case, steady state analysis was done. A slice of the domain, which corresponds to 1/32 of total with 11.25°, is used for numerical modelling, due to periodic symmetry of the model. The Figure 3.9 and Figure 3.10 shows the total domain and the focused slice.

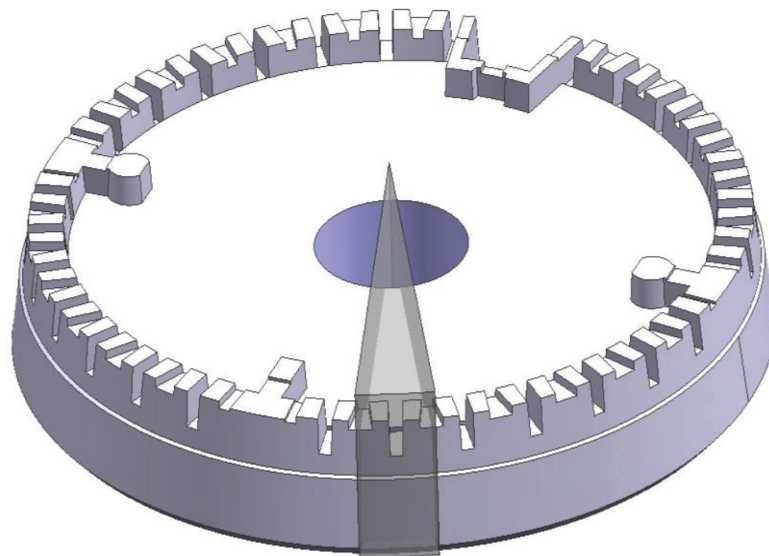


Figure 3.9. Burner slice to create the domain

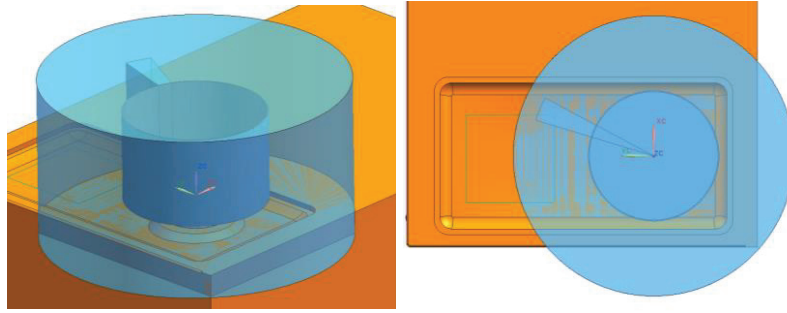


Figure 3.10. Domain with the taken slice. Trimetric and top views

It can be seen that, pan support was also excluded from the data. This was due to geometric limitations after considering only a slice of the domain. The loading height of the pot remains as it is supposed to be with pan support. The pot is modelled according to requirements of related European Norms. Figure 3.11 shows the final state of the domain.

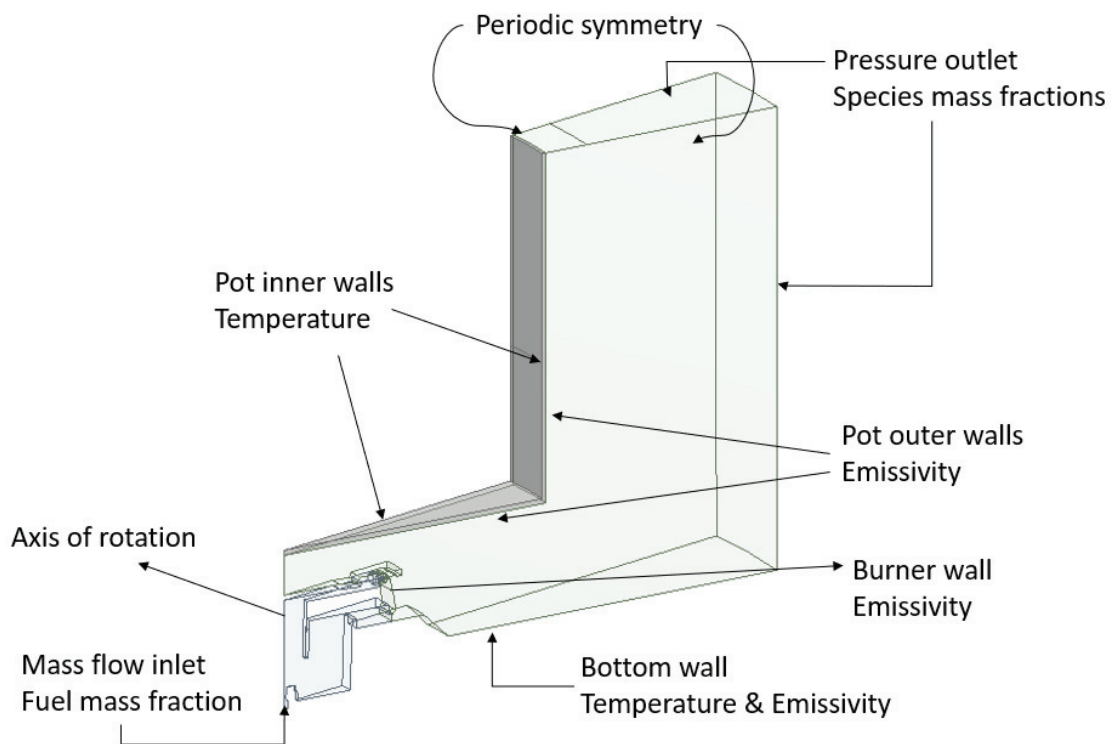


Figure 3.11. Domain slice

In Figure 3.11, it can be seen that the burner body, flame spreader, hob sheet and burner lid are taken as walls in the domain.

Meshing is a crucial part in numerical modelling. The quality of the mesh may have big impact on the results of the calculations. For a complex geometry such as it is in this study, some simplifications had to be done to improve mesh quality. The hob sheet has been turned into flat surface, unnecessary radiuses and small details which would not have a significant impact on results are cancelled. Choosing the proper slice is important to not interact with anything, which would cause problem with matching side surfaces. It is important to be able to define a periodic symmetry of the domain, so that to mimic the whole domain. The mesh element size is reduced especially in the critical zones like injector surface, flame spreader ports and pot region. To reduce the computational costs, polyhedral meshing is used. Studies show that this meshing method is accurate for complex geometries and it reduces computational effort by decreasing cell numbers [22,24]. The model was first meshed with tetrahedral cells, then turned into polyhedral cells in Fluent. Table 3.7 shows the number of cells for tetrahedral and polyhedral elements.

Table 3.7. Change in numbers of cells between tetrahedral and polyhedral meshing for the domain

Case Number	Cell Number (Tetrahedral)	Cell Number (Polyhedral)
1st	141190	42118
2nd	330941	91581
3rd	737600	186176

As it is shown in table, turning the domain into polyhedral cells reduces the number of elements 3 to 4 times.

Internal circulation of water and evaporation is neglected since it is not feasible to model water. The simulation involved in this study will correspond to a process, where the inner temperature of the pot surface would be constant as in the case of boiling water. Since the numerical model does not simulate the exact experiments, which were mentioned in earlier topics, percentage changes in results can be compared between model predictions and experiments instead of exact values.

After building the mesh and setting up the domain for simulation, it is important to choose correct models for numerical calculations. Fluent provides many options for several models for different kind of problems. That is why in some cases, there may be

more than one accurate model for the problem. To define the flow type, the fuel flow rate is measured experimentally. Reynolds number of injector is calculated as:

$$Re = \frac{\rho VD}{\mu} = \frac{VD}{\nu} \quad (3.35)$$

where ρ , V , D , μ and ν are density, velocity of the fuel, injector diameter, dynamic viscosity and kinematic viscosity, respectively. It is important to know that injector design is crucial in defining the flow type, as injector has diameter changes through vertical axis. Reynolds number changes with change in injector's inner diameter, flow rate and fuel temperature because of changes in properties. Reynolds number of methane in this aspect changes between 2680 and 5680, depending on flow rate, for test requirement. However, the turbulent flow is observed only in the narrow zone of the injector. In the injector outlet, the flow is transitional. Similarly, Reynolds number in burner port is 510, which shows that flow in burner outlet is laminar. For this case, Fluent offers a three-equation laminar-turbulent transition k-kl- ω model to solve turbulent kinetic energy (k_T), laminar kinetic energy (k_L) and the scale determining variable (ω) [25]. The model equations are:

$$\frac{Dk_T}{Dt} = P_{k_T} + R_{BP} + R_{NAT} - \omega k_T - D_T + \frac{\partial}{\partial x_j} \left[\left(\nu + \frac{\alpha_T}{\sigma_k} \right) \frac{\partial k_T}{\partial x_j} \right] \quad (3.36)$$

$$\frac{Dk_L}{Dt} = P_{k_L} - R_{BP} - R_{NAT} - \omega k_T - D_L + \frac{\partial}{\partial x_j} \left[\nu \frac{\partial k_L}{\partial x_j} \right] \quad (3.37)$$

$$\begin{aligned} \frac{D\omega}{Dt} = & C_{\omega 1} \frac{\omega}{k_T} P_{k_T} + \left(\frac{C_{\omega R}}{f_W} - 1 \right) \frac{\omega}{k_T} (R_{BP} + R_{NAT}) - C_{\omega 2} \omega^2 + C_{\omega 3} f_{\omega} \alpha_T f_W^2 \frac{\sqrt{k_T}}{d^3} \\ & + \frac{\partial}{\partial x_j} \left[\left(\nu + \frac{\alpha_T}{\sigma_{\omega}} \right) \frac{\partial \omega}{\partial x_j} \right] \end{aligned} \quad (3.38)$$

The various terms in the model equations represent production, destruction and transport mechanisms [25]. Fluent suggests not to change model constants for the related transition model.

Although the CFD software has premixed and partially premixed combustion models available, these models are only valid for turbulent, subsonic flows. As an alternative, the species transport model and finite rate chemistry are available in the software. When species transport model is used to solve conservation equations for chemical species, the software predicts the local mass fraction of each species, Y_i , through the solution of a convection-diffusion equation for the i^{th} species [29]. The equation takes the following general form:

$$\frac{\partial}{\partial t}(\rho Y_i) + \nabla \cdot (\rho \vec{v} Y_i) = -\nabla \cdot \vec{J}_i + R_i + S_i \quad (3.39)$$

where R_i is the net rate of production of species i by chemical reaction and S_i is the rate of creation by addition from the dispersed phase plus any user-defined sources [29]. \vec{J}_i is the diffusion flux of species i . Mass diffusion computation depends on the flow type.

For methane-air mixture, two step reaction mechanism, which involves three reactions and 6 species is chosen [27]. The reaction steps are shown in Table 3.8.

Table 3.8. Reactions for 2-step reduced mechanism in Fluent

Reaction Number	Reaction
1st	$CH_4 + 1.5O_2 \rightarrow CO + 2H_2O$
2nd	$CO + 0.5O_2 \leftrightarrow CO_2$

To take radiation into account for more accurate heat transfer calculation, discrete ordinates radiation model is used. This model is recommended to give accurate results in complex geometries and in addition, computational costs are not so high. The model solves the equation for radiation intensity for a set of discrete directions which span the total solid angle range of 720 degrees around a point in space. As it is described, “*this radiation model solves the radiative transfer equation for a finite number of discrete solid*

angles, each associated with a vector direction \vec{s} fixed in the global Cartesian system (x, y, z)” [29]. The absorption coefficient is modeled with weighted sum of gray gases model (WSGGM). Enabling this model is important to take absorption of CO₂ and H₂O into account, so that radiative heat transfer prediction would be more accurate [11].

Defining correct boundary conditions is another crucial part of numerical modelling. The walls of the domain, which are exposed to ambient were treated as pressure outlets. The atmospheric pressure inside the Fluent was defined as 0 atm as it is relative pressure in the software. Fuel inlet was defined as mass flow inlet, which was measured experimentally for each test process. Mass fractions of species were defined to the boundaries. For heat transfer calculations, the inner wall of the pot was divided into two zones. First zone represents the surface which is in the same level of water height inside the pot. Constant wall temperature was defined as 25 K higher than the water temperature [11]. This temperature varies for combustion or efficiency test cases. The second zone represents the pot surface which is in contact with convective air. Temperature and convective heat transfer coefficient were defined to the surface. The experimentally measured temperature values and convective heat transfer coefficient are defined to the walls which represent the hob sheet. Gravitational forces are also enabled to take buoyancy driven flow around the pot into account.

Final solutions were gained in two steps, as it is suggested for combustion problems in complex geometries. First, energy equation and reactions were switched off to simulate the mixture flow. Then energy equation and reactions were switched on and high temperature patch was performed to simulate ignition of the mixture to get results. Solutions are assumed converged when heat flux and pollutant emissions remained nearly constant, which usually happens over 500-1000 iterations.

CHAPTER 4

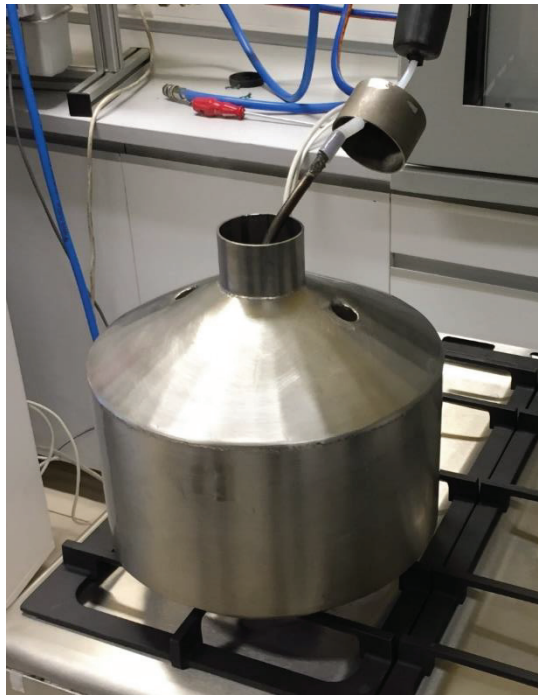
RESULTS AND DISCUSSIONS

In this chapter results of experimental and numerical studies will be presented. The tests were performed according to related European Norms for both combustion and efficiency cases. Combustion test was only performed for combustion test number 1, which is the representative of the test performed with reference gas, at maximum gas inlet pressure with full on knob position. Numerical studies were first performed to validate the model with experimental measurements. Then mesh dependency of the model was observed. In the end, loading height of the pot was changed to see its effects on pollutant emission rates and thermal efficiency. In total, six different experiment has been performed. Similarly, three numerical modelling for validation, three for mesh dependency and ten modelling to observe effects of changing loading height in combustion and efficiency test cases have been performed.

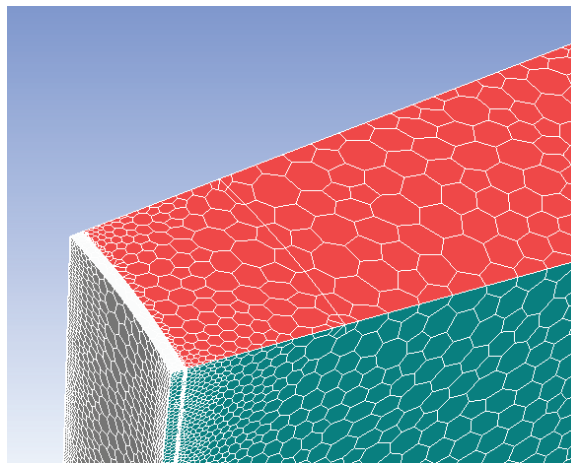
4.1. Preliminary Results and Model Validation

First study is done for combustion case to see the performance of the numerical model in terms of species reactions and temperature distribution. The prototype appliance was run with G20 reference gas, which corresponds to methane, at 25 mbar fuel inlet pressure for combustion test.

In experimental setup, the commercially available analyzer gets sample from flue gas and displays the water-free volumetric concentration of CO and CO₂. To be able to model the same conditions, a surface on top boundary was modeled as it would correspond to section of the hood to measure concentration of pollutants (as shown in Figure 4.1). However, modelling the surface with same dimensions as hood is not enough, since Fluent takes water vapor into account too. To extract water vapor from the total, a dry analysis was performed to get water-free concentration results.



a)



b)

Figure 4.1. Hood a) the usage in test and b) corresponding surface

Temperature contour (as shown in Figure 4.2) shows temperature distribution. As it can be seen, the temperature region beyond 2000 K occurs at the outlet of the burner port, which corresponds to blueish flame cone region of the flame. Temperature distribution seems to be well calculated by the model, comparing with the calculation of adiabatic flame temperature, which was described in chapter 3.

Even if the temperature distribution was well predicted by the model, pollutant emission results show that there are major differences between experimental and

numerical study in terms of CO and CO₂ fractions. Table 4.1 shows the results of experiment and Fluent.

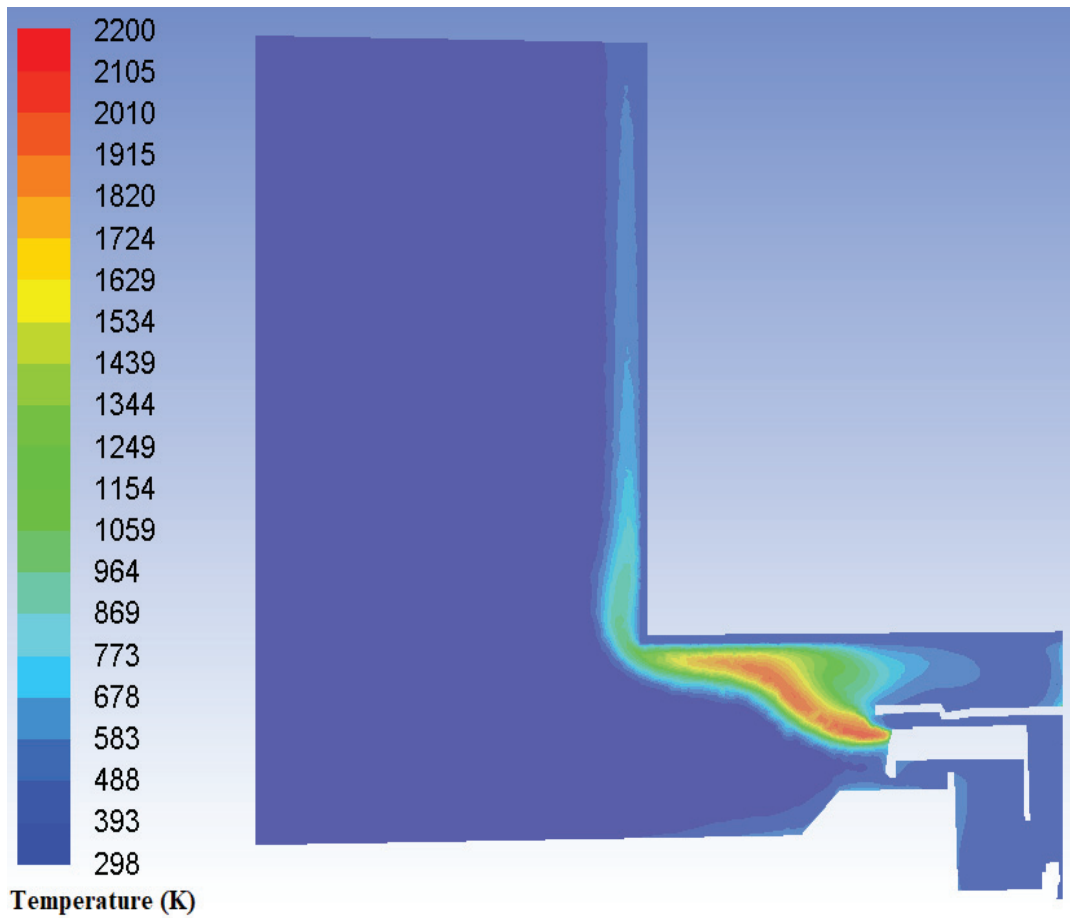


Figure 4.2. Temperature distribution in the midplane of domain for methane combustion

Table 4.1. Water-free results from Fluent and experiment

Species	Fluent Results (%)	Experimental Results (%)
CO ₂	1.746	4.4
CO	0.0810	0.0228

As it was seen, CO volumetric fraction was overpredicted by the model, just as CO₂ fraction was underpredicted. There are many reasons that would help explaining the difference in the results.

4.1.1. Effects of Pan Support and Hob Sheet Design

As described earlier, the pan support was not included to the numerical model since it would require modelling the whole domain, which would create a big computational cost. In addition to this, the effect of depth of the pool that holds the burners is neglected for the same reason. Both neglected effects create differences in the air flow to the burner. To verify this, another experiment was performed with different cooktop, where the pool depth is narrower, fingers of pan support are less and thinner, but the burner and injector are the same. The differences in the design and results are shown in Figure 4.3 and Table 4.2, respectively.

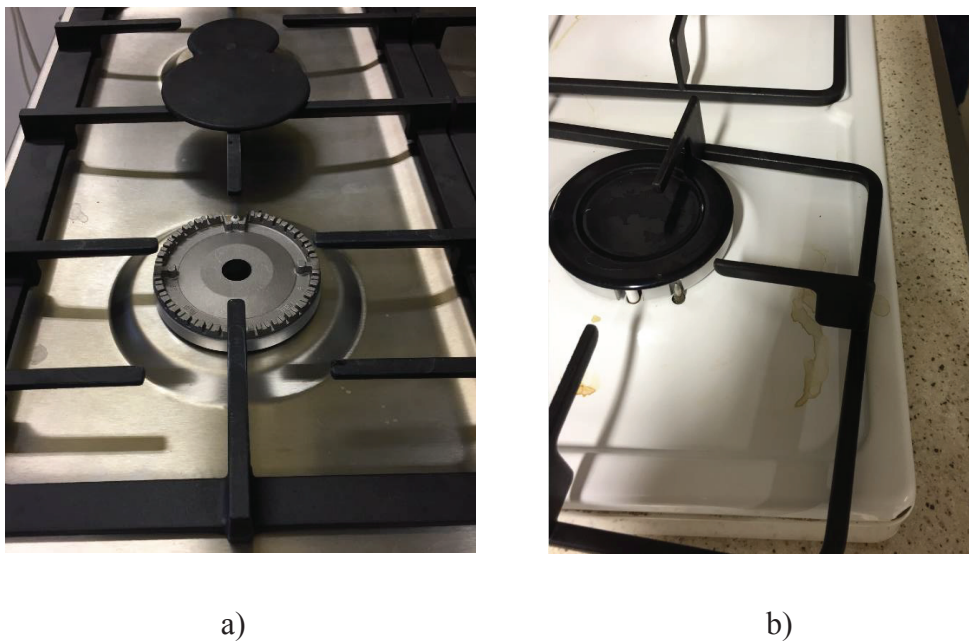


Figure 4.3. Difference in hob design and pan support for appliances a) deep pool with 2-finger pan support b) narrow pool with 1-finger thin pan support

Table 4.2. Combustion test results from appliance a and appliance b

Species	Appliance a	Appliance b
CO ₂ (%)	4.4	3.73
CO (%)	0.0228	0.0086

Decrease of both volumetric fraction of CO and CO₂ are related with increase of O₂. This shows that air entrainment to burner body increases as pool depth and number of fingers decrease.

It should be noted that pan support also has negative effect on thermal efficiency, since a portion of the released heat would be lost to heat up the pan support. To observe this effect, efficiency case is tested with same appliance, same loading height (35.5 mm), same burner, same flow rate but different number of fingers per each burner on pan support. Figure 4.4 shows the difference between the tested pan supports and Table 4.3 shows the test results.

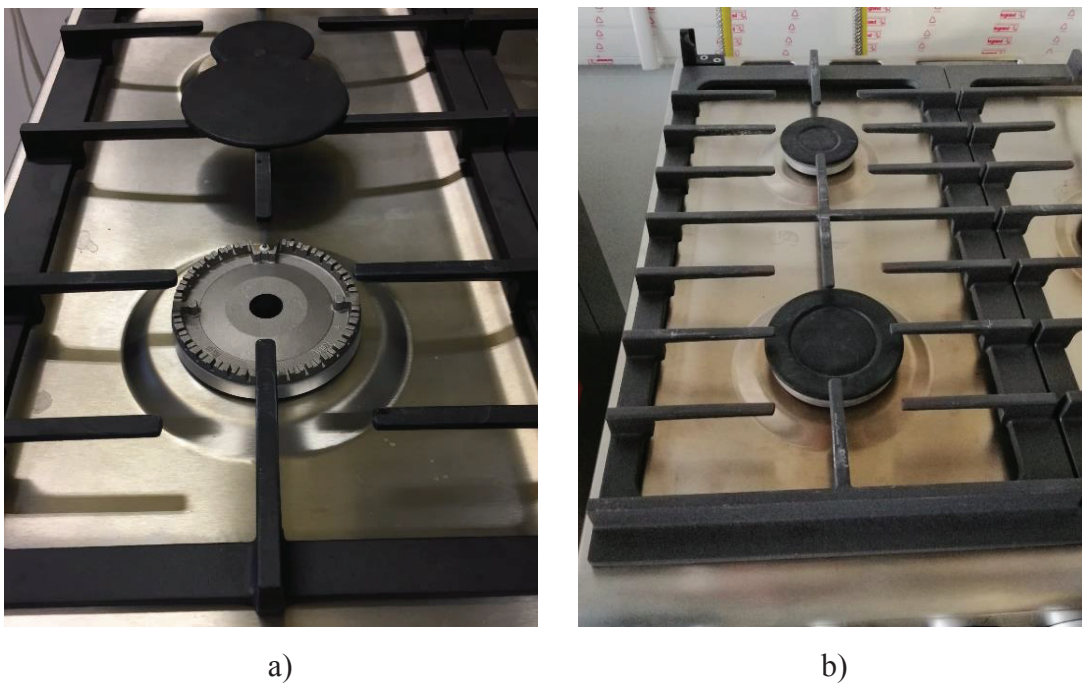


Figure 4.4. Difference in pan support a) 2-finger model b) 3-finger model

Table 4.3. Efficiency test results from pan support a and pan support b with $\pm 0.9\%$ error tolerance from measurement uncertainties

	2-Finger Pan Support	3-Finger Pan Support
Efficiency (%)	57.4	53.9

4.1.2. Effect of Reduced Reaction Mechanism

It is known that combustion mechanism of methane includes hundreds of reaction steps and tens of sub-species. Since it is not feasible to use the real mechanism in terms of computational cost, simplified reaction mechanisms were developed to have a limited number of species and reaction steps, which helps reducing the computation time and effort. However, as the mechanisms are simplified, the accuracy of concentrations of species decrease. The studies are available in the literature that investigates the performance of these type of mechanisms [27,28] reduced mechanisms available in literature that give results in acceptable accuracy, such as GRI-Mech 3.0, which consists of 325 reactions and 53 species. However, it is not feasible to use such a mechanism in a computer that is built for domestic use.

With constrains of computational availability and geometry, the numerical model still needed to be validated. For this cause, a set of experiments and numerical calculations were performed. To see if the results follow the same trend, flow rate of the fuel was changed, and the other parameters were kept constant in both experiments and numerical calculations. The results are shown in the Figure 4.5 and Figure 4.6.

For the cases with fuel flow rate 0.153, 0.318 and 0.372 m³/h, air to fuel equivalence ratio λ is 0.37, 0.47 and 0.42, respectively. As it is seen in Figure 4.4 and Figure 4.5, the experimental and numerical results follow a similar trend. An increase or decrease of fuel flow rate means velocity change. This also causes change in air entrainment force and increase or decrease of airflow rate into the burner body. However, the volume fraction of air and fuel is not the only parameter. As fuel flow rate changes, flow characteristic of the fuel changes and with this effect, homogeneity of the mixture changes, since the burner is a partially premixed burner. Additionally, with changing flow rate, flame length changes and this changes the characteristics of post flame reactions near the flame surface.

When the fuel flow rate is increased from 0.153 m³/h to 0.318 m³/h, the rate of unburnt fuel inside the flame increases and flame tend to be characterized more as non-premixed flame, as the reactions only take place at the surface of the flame, by the oxygen diffusion from atmosphere. Although the reason of increase in CO and CO₂ concentrations can be explained by the flow rate increase, it can be seen that a further

increase of flow rate from 0.318 m³/h to 0.372 m³/h did not cause a similar increase in pollutant concentrations. Instead, a slight decrease of concentrations is observed both experimentally and numerically. This can be explained with same reasons, as increasing flow rate changes turbulence, homogeneity and flame length. As it can be seen from the lambda values, a further increase fuel flow rate did not cause a proportional increase in primary air entrainment in injector outlet, which cause change in concentrations of species and homogeneity of mixture. This is also valid for secondary air, which is entrained after burner port region. However, it should also be noted that an increase or decrease in air entrainment does not necessarily mean a linear change in homogeneity results. The entrained air may not be mixed with unburnt gas in reaction and post flame regions. While change in homogeneity of mixture affects combustion results, having an increase in secondary air will cause reduction of rate of pollutant concentrations. It should be noted that, as this type of partially premixed burners cannot be fully controlled in terms of fuel/air mixture, burner manufacturers mainly focus on the burner's performance in operating gas supply pressure ranges while designing a burner. This is mainly because the standard requires success criteria for gas supply limit pressure values. In any case, the results show that the change trend for experimental and numerical tests is similar and this would be used to evaluate changes in percentage and compare different cases.

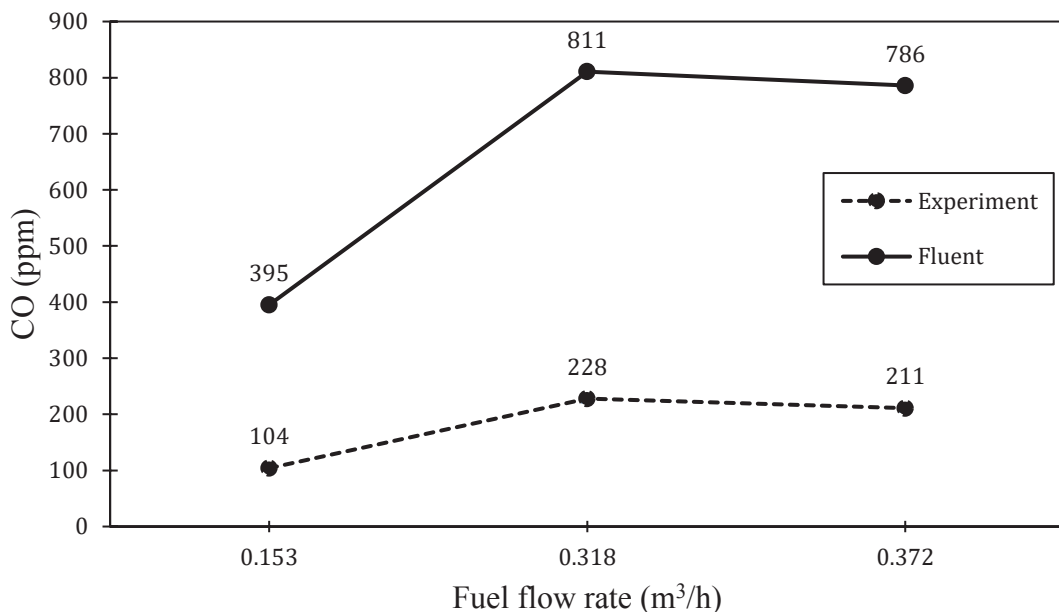


Figure 4.5. Change of CO concentrations with changing gas flow rate

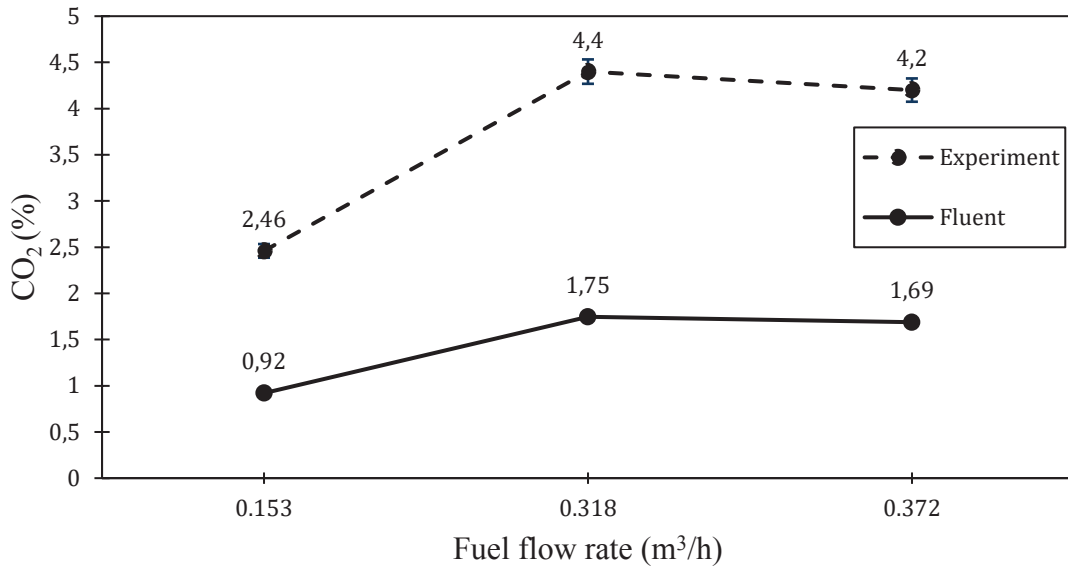


Figure 4.6. Change of CO₂ concentrations with changing gas flow rate

4.2. Mesh Dependency

After evaluation of the preliminary results, the model's mesh dependency was checked. As this model includes both solid and fluid region in a complex geometry, the focus of increasing and decreasing the number of elements was the crucial zones, such as pot part, injector, burner body, flame spreader and close surroundings of the burner. Table 4.4 shows the change rate of results with the number of mesh elements.

Table 4.4. Mesh dependency

No. of Elements	Parameter			$[X_{n+1}-X_n] / X_n$		
	CO ₂ (%)	CO (%)	Heat Transfer to Pot (W)	CO ₂ (%)	CO (%)	Heat Transfer to Pot (%)
42118	1.443	0.0629	48.17	3.6	10	0.85
91581	1.495	0.0692	48.58	2.87	5.2	0.93
186176	1.538	0.0728	48.13	1.23	1.24	1.2
348271	1.557	0.0719	47.55			

Domain with 186176 elements was chosen to make progress, as the change rate in results decreased below 5%.

4.3. Effects of Loading Height

After numerical model was decided to be mesh independent, effects of loading height were observed for both pollutant concentrations and thermal efficiency. To observe both parameters, both efficiency and combustion test models were used with pot inner diameter of 260 mm and 220 mm, respectively. The definition of loading height is shown in Figure 4.7. Figure 4.8 shows the thermal efficiency case results from numerical model for varying loading height.

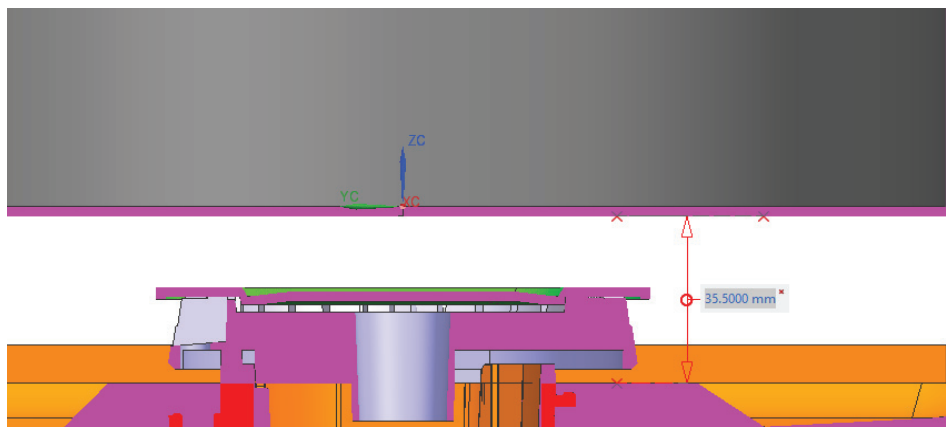


Figure 4.7. Loading Height

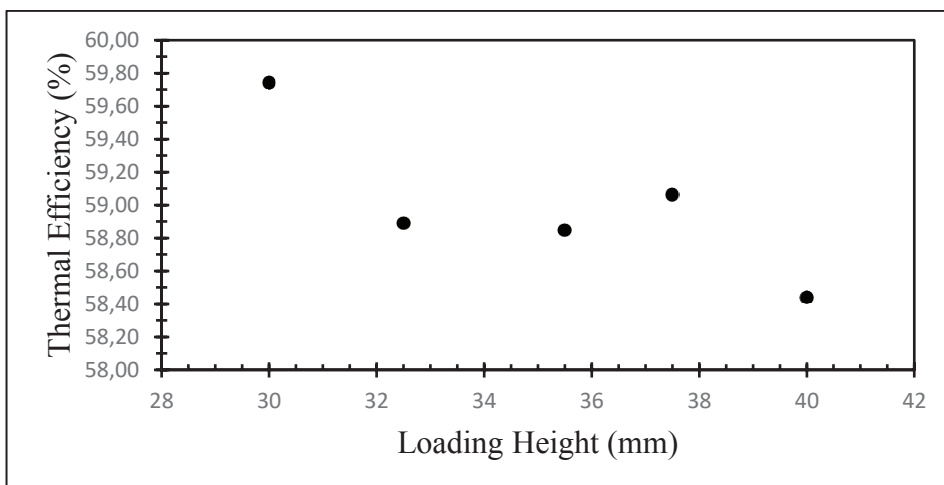


Figure 4.8. Change in thermal efficiency with loading height

As the loading height increases, heat loss to environment is also expected to increase, which will cause a decrease in thermal efficiency. However, change in loading height may also affect the flame impingement angle, which will change the flame contact region through the diameter of the pot. As the loading height increases, flame may be positioned normal to the pot surface, which would cause the flame contact region to move closer to center of the pot. This would also increase the contact time of high temperature zone of flame before it is cooled down by atmosphere or rise along the vertical surface of the pot, which will cause an increase in thermal efficiency. Figure 4.9 shows a representative surface heat flux distribution through the pot.

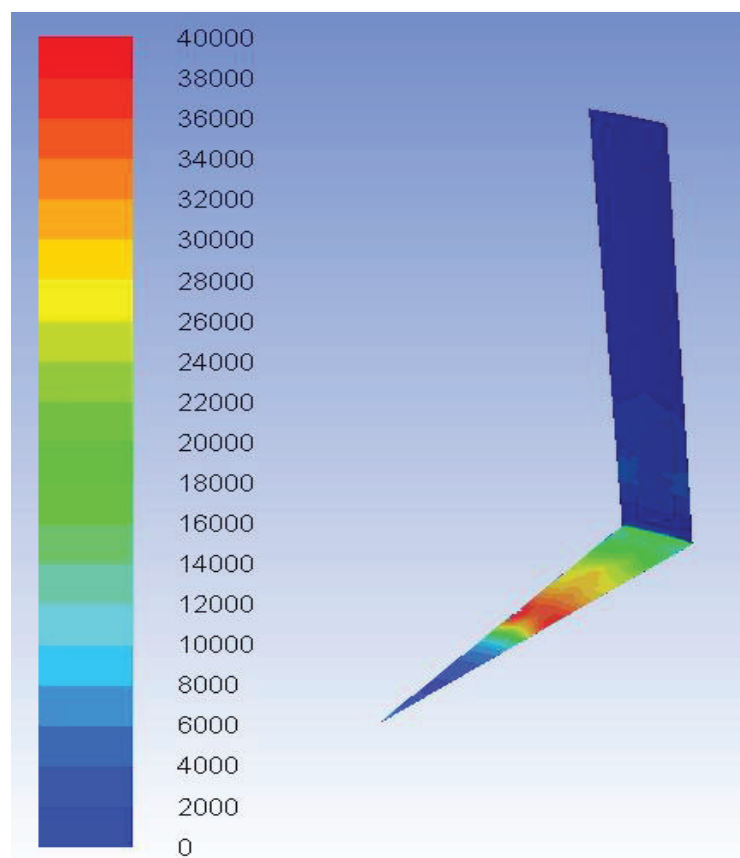


Figure 4.9. Contour of pot surface heat flux

To gain a better insight, Figure 4.10 shows the difference in heat flux distribution along bottom surface of the pot between 30mm and 40mm loading heights.

Figure 4.11 shows the results of CO₂ and CO changes with loading height in numerical model.

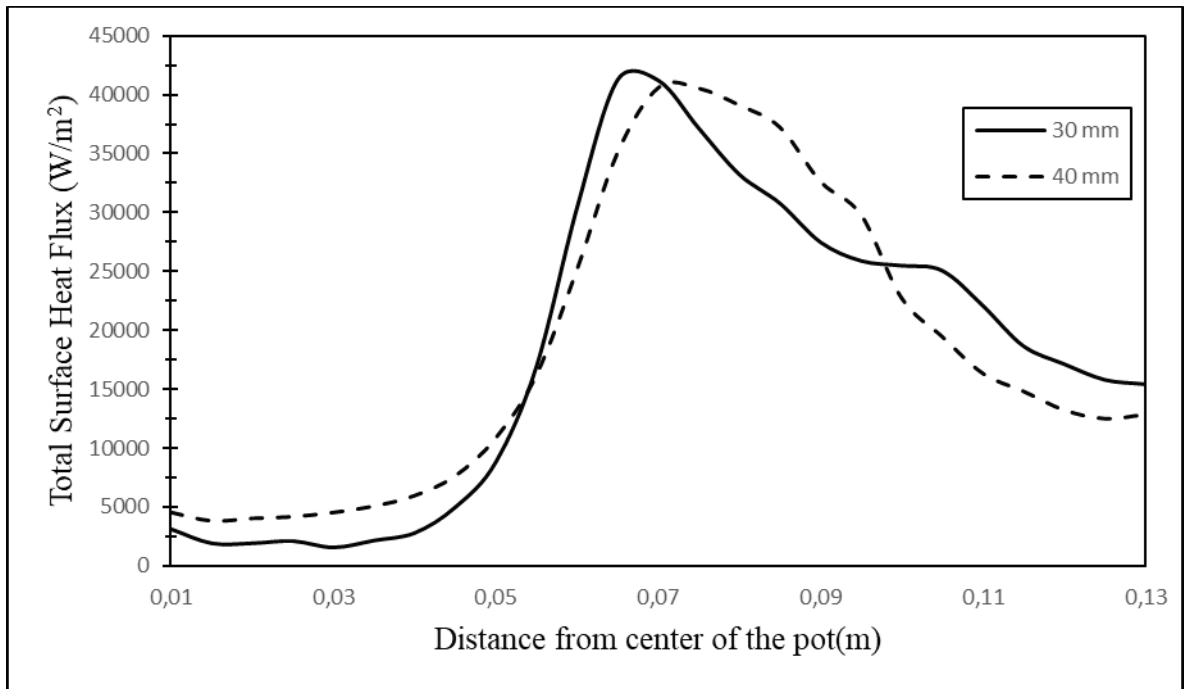


Figure 4.10. Heat flux distribution on bottom surface of the pot

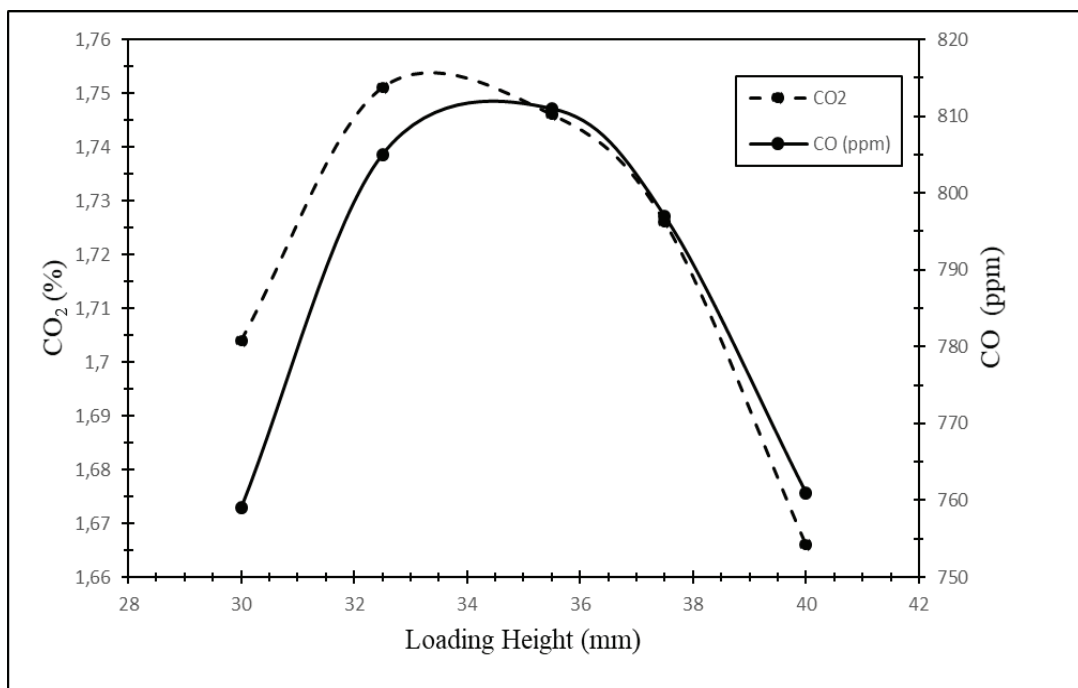


Figure 4.11. Changes in CO₂ and CO concentrations with loading height

The reduction in emission rates after increasing loading height can be explained with post flame reactions. In partially premixed burners, reactions keep taking place with secondary air. Taking 35.5 mm height as reference, if more gap is provided, an increase in rate of oxygen is expected. If there is more oxygen to turn CO into CO₂, an increase in

rate of CO₂ and a decrease in CO would be expected. Depending on the entrained air, this may also result in a decrease of both CO and CO₂ rate, if reaction rate will be lower than the provided oxygen rate. However, the conditions may change for reducing the height. Although it would be expected to see an increase in pollutant emissions with same approach, it is also possible to see a decrease in rate of pollutants, as we reduce the loading height. This may be a result of a decrease in heat output. With decreasing the loading height, post flame reaction rate decreases with a decrease of air entrainment. This can be a result of change in flame shape. A decrease in post flame reaction rate will also result in an increase in unburnt fuel rate. That supports the idea of a decrease in heat output. As an example, Table 4.5 shows result of numerical calculation for mole fraction of CH₄ in hood surface. Although CO and CO₂ levels decreases with reducing the loading height from 35.5 mm to 30 mm, this results in a decrease of burning efficiency, as it is mentioned in equation 3.7.

Table 4.5. Mole fraction of CH₄ for numerical combustion case model for 30 and 35.5mm loading heights.

Loading Height (mm)	Mole Fraction of CH ₄
30	0.038%
35.5	0.02%

CHAPTER 5

CONCLUSION AND FUTURE WORK

In this study, it is aimed to improve pollutant emission rates and/or thermal efficiency of domestic gas cooktop burners. For this cause, first a theoretical insight had to be gained over the domestic gas burner systems. While aiming for an improvement study, it is inevitable to consider requirements of standards, as appliance manufacturers must meet necessities to get necessary certifications. If the test procedures would be ignored, there might be a possibility to offer a configuration, which would potentially fail at the requirements of the norms. For this reason, the experimental tests were performed according to test procedures, and numerical model was built accordingly. It was aimed to use numerical model to see effects of changing parameters on thermal efficiency and pollutant emissions. However, due to limited computational opportunities, some simplifications and assumptions had to be done. Using a reduced mechanism for chemical reactions and modelling only a part of the domain for a periodic symmetry boundary condition were crucial at this point. The results can be summarized as follows:

Although the volumetric fractions of CO and CO₂ are not accurate with test results, thermal efficiency is well predicted by the reduced mechanism. With this, it can be said that temperature field and dynamics of the flame are accurate. Even if the pollutant concentrations are not accurate, with several numerical model and experiments, it was validated that a comparison could be done between the results. With this approach, the current loading height of 35.5 mm was offered to be decreased to 30 mm to improve thermal efficiency and pollutant concentrations at the same time. Considering all the numerical and geometric assumptions, this suggestion must be validated with an experiment, with a suitable pan support.

As future work, as it was seen with experimental and numerical studies, to improve accuracy of the numerical results of CO and CO₂ fractions, a more detailed reaction mechanism must be used. More detailed reaction mechanisms increase computational effort dramatically. To give an example, with same computational source, using GRI Mech 2.11 reaction mechanism, which includes 277 reactions and 49 species,

increases computational effort 20 times. Nevertheless, this will help gaining a much better insight to study over reducing the carbon emissions to environment. In addition, to reduce the number of assumptions, modelling a significantly bigger domain will be considered. This will help including the effects of pan support into the numerical model and provide a better approach.

REFERENCES

1. United States Environmental Protection Agency. Indoor Air Quality <https://www.epa.gov/indoor-air-quality-iaq/protect-indoor-air-quality-your-home> (accessed Jan 11, 2018).
2. National Ambient Air Quality Standards for Carbon Monoxide, Integrated Science Assessment for Carbon Monoxide (Final Report), U.S. Environmental Protection Agency, Washington, DC, 2010
3. Integrated Science Assessment for Oxides of Nitrogen - Health Criteria (2016 Final Report), U.S. Environmental Protection Agency, Washington DC, 2016
4. European Environmental Agency. Environment and Health: Indoor Air Pollution <https://www.eea.europa.eu/signals/signals-2013/infographics/indoor-air-pollution/view> (accessed April 21, 2018)
5. Moschandreas, D.J.; Zabransky Jr., J. Spatial Variation of Carbon Monoxide and Oxides of Nitrogen Concentrations Inside Residences. *Environment International* **1982**, 8 (1), 177 – 183
6. Garrett, M. H.; Hooper, M. A.; Hooper, B. M., Nitrogen Dioxide in Australian Homes: Levels and Sources. *Journal of the Air & Waste Management Association*, **1999**, 49 (1), 76-81
7. Singer, B.C.; Pass, R.Z.; Delp, W.W.; Lorenzetti, D.M.; Maddalena, R.L., Pollutant Concentrations and Emission Rates from Natural Gas Cooking Burners without and with Range Hood Exhaust in Nine California Homes. *Building and Environment* **2017**, 122, 215 - 229
8. Hou, S.-S.; Lee, C.-Y.; Lin, T.-H., Efficiency and Emissions of a New Domestic Gas Burner with a Swirling Flame. *Energy Conversion and Management* **2007**, 48 (5), 1401 - 1410
9. Ko, Y.-C.; Lin, T.-H., Emissions and Efficiency of a Domestic Gas Stove Burning Natural Gases with Various Compositions. *Energy Conversion and Management*, **2003**, 44 (19), 3001 - 3014
10. Sumrerng, J.; Rungsimuntuchart, N., High Efficiency Heat-recirculating Domestic Gas Burners. *Experimental Thermal and Fluid Science*, **2002**, 26 (5), 581 - 592
11. Boggavarapu, P.; Ray, B.; Ravikrishna, R. J. F., Thermal Efficiency of LPG and PNG-fired Burners: Experimental and Numerical Studies. *Fuel*, **2014**, 116, 709-715.
12. Hou, S.-S.; Ko, Y.-C., Effects of Heating Height on Flame Appearance, Temperature Field and Efficiency of an Impinging Laminar Jet Flame Used in Domestic Gas Stoves. *Energy Conversion and Management* **2004**, 45, 1583-1595

13. Hou, S.-S.; Ko, Y.-C., Influence of Oblique Angle and Heating Height on Flame Structure, Temperature Field and Efficiency of an impinging Laminar Jet Flame. *Energy Conversion and Management*, **2005**, 46, 941-958
14. Karunanithy, C.; Shafer, K., Heat Transfer Characteristics and Cooking Efficiency of Different Sauce Pans on Various Cooktops. *Applied Thermal Engineering*, **2016**, 93, 1202 - 1215
15. Li, H.B.; Wong, T.T.; Leung, C.W.; Probert, S.D., Thermal Performances and CO Emissions of Gas-fired Cooker-top Burners. *Applied Energy*, **2006**, 83 (12), 1326 - 1338.
16. El-Mahallawy, F.; Habik, S.E.D., Fundamentals and Technology of Combustion, 1st ed.; Elsevier Science, 2002
17. Jones, H.R.N., The Application of Combustion Principles to Domestic Gas Burner Design. Taylor & Francis: 1989
18. Gattei, L. A Study on the Fluid Dynamics of Domestic Gas Burners. PhD. Dissertation, Universita Di Bologna, 2008
19. C.E.N. Domestic cooking appliances burning gas – Part1–1: Safety – General. European Standard EN 30-1-1, 2013
20. C.E.N. Domestic cooking appliances burning gas – Part2-1: Rational use of energy – General. European Standard EN 30-2-1, 2015
21. Massachusetts Institute of Technology. Thermodynamics Notes <https://web.mit.edu/16.unified/www/FALL/thermodynamics/notes/node111.html> (accessed Aug 24, 2018)
22. Symscape Polyhedral, Tetrahedral, and Hexahedral Mesh Comparison <https://www.symscape.com/polyhedral-tetrahedral-hexahedral-mesh-comparison.html> (accessed Apr 18, 2018)
23. Sosnowski, M.; Krzywanski, J.; Gnatowska, R., Polyhedral Meshing as an Innovative Approach to Computational Domain Discretization of a Cyclone in a Fluidized Bed CLC unit. *E3S Web of Conferences*, **2017**, 14.
24. Spiegel, M.; Redel, T.; Jonathan Zhang, Y.; Struffert, T.; Hornegger, J.; Grossman, R.; Doerfler, A.; Karmonik, C., Tetrahedral vs. Polyhedral Mesh Size Evaluation on Flow Velocity and Wall Shear Stress for Cerebral Hemodynamic Simulation. *Computer Methods in Biomechanics and Biomedical Engineering*, **2011**, 14, 9-22.
25. Keith Walters, D.; Cokljat, D., A Three-Equation Eddy-Viscosity Model for Reynolds-Averaged Navier–Stokes Simulations of Transitional Flow. *Journal of Fluids Engineering*, **2008**, 130

26. Raithby, G.D.; Chui, E., A Finite-Volume Method for Predicting a Radiant Heat Transfer in Enclosures With Participating Media. *Journal of Heat Transfer*, **1990**, 112, 415-423.
27. Bibrzycki, J.; Poinso, T.; A, Z., Investigation of Laminar Flame Speed of CH₄/N₂/O₂ and CH₄/CO₂/O₂ Mixtures Using Reduced Chemical Kinetic Mechanisms. *Arch Combust* **2010**, 30
28. Anetor, L.; Osakue, E.; Odetunde, C., Reduced Mechanism Approach of Modeling Premixed Propane-Air Mixture Using ANSYS Fluent. *Engineering Journal* **2012**, 16
29. ANSYS, Inc. **2019**. *Fluent 17: User Guide*. Canonsburg, PA, USA.